Combinatorics of rectangulations: Old and new bijections

Andrei Asinowski[*], Jean Cardinal[†], Stefan Felsner[‡], Éric Fusy[§]

April 8, 2024

A rectangulation is a decomposition of a rectangle into finitely many rectangles. Via natural equivalence relations, rectangulations can be seen as combinatorial objects with a rich structure, with links to lattice congruences, flip graphs, polytopes, lattice paths, Hopf algebras, etc. In this paper, we first revisit the structure of the respective equivalence classes: *weak rectangulations* that preserve rectangle–segment adjacencies, and *strong rectangulations* that preserve rectangle–rectangle adjacencies. We thoroughly investigate posets defined by adjacency in rectangulations of both kinds, and unify and simplify known bijections between rectangulations and permutation classes. This yields a uniform treatment of mappings between permutations and rectangulations that unifies the results from earlier contributions, and emphasizes parallelism and differences between the weak and the strong cases. Then, we consider the special case of *guillotine rectangulations*, and prove that they can be characterized — under all known mappings between permutations and rectangulations — by avoidance of two mesh patterns that correspond to "windmills" in rectangulations. This yields new permutation classes in bijection with weak guillotine rectangulations, and the first known permutation class in bijection with strong guillotine rectangulations. Finally, we address enumerative issues and prove asymptotic bounds for several families of strong rectangulations.

Contents

[*]Alpen-Adria Universität Klagenfurt, Austria. E-mail: andrei.asinowski@aau.at
[†]Université libre de Bruxelles, Belgium. E-mail: jean.cardinal@ulb.be
[‡]Technische Universität Berlin, Germany. E-mail: felsner@math.tu-berlin.de
[§]LIGM, CNRS, Univ. Gustave Eiffel, Marne-la-Vallée, France. E-mail: eric.fusy@u-pem.fr

1 Introduction

A *rectangulation* is a decomposition of a rectangle into finitely many interior-disjoint rectangles. Rectangulations constitute a classical topic in mathematical tessellation theory. Among the earliest contributions on this topic one finds two papers by Abe from early 1930s [1, 2], and the papers by Brooks, Stone, Smith, and Tutte (collectively known as *Blanche Descartes*) on "squaring the square" [22], and on partitioning a square into equal-area rectangles [33]. In the last decades, many results on rectangulations have been published in journals and conferences on computational geometry as well as engineering and electronics, due to their being a basic model in *floorplanning* — an essential step in the design of very large scale integrated circuits (VLSI) [71, 67, 28]. In floorplanning, functional blocks of a circuit, represented by rectangles, have to be packed on a small rectangular area. The term *floorplan* is therefore often used to designate a rectangulation. Rectangulations have also applications in the analysis of geometric algorithms [11, 25], in visualization of scientific data (for instance treemaps [12] and cartograms [82, 23]), in mathematical foundations of architectural design [76], and also appear in visual art — notably in the work of the Dutch art movement *De Stijl*, see Figure 1.

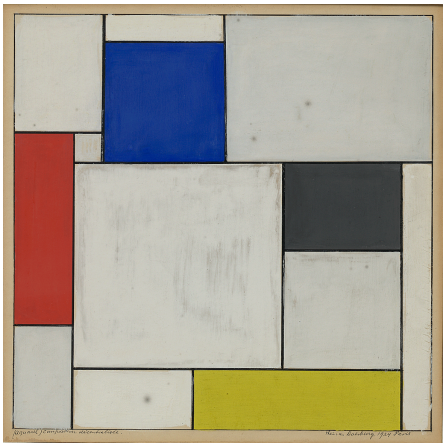

Figure 1: Artwork *Composition décentralisée* (1924) by Theo van Doesburg (Dutch, 1883–1931). Solomon R. Guggenheim Museum, New York.

We investigate structural properties of rectangulations, which in particular means that we are not interested in precise measures of rectangles but rather in adjacencies between their elements — rectangles and segments. In order to treat rectangulations as combinatorial objects, one can introduce an equivalence relation formalizing the idea of two rectangulations being "structurally identical". There are two natural equivalence relations of this kind. The *weak equivalence* preserves incidence and sidedness between segments and rectangles. The *strong equivalence* additionally preserves the adjacencies between rectangles. Precise definitions are given in Section 2.2.

Many structural investigations of rectangulations are focused on their bijective representation by classes of permutations determined by pattern avoidance [3, 46, 41, 53, 66, 6, 26, 56, 57, 59]. For example, *Baxter permutations*, defined by avoidance of a certain pair of *vincular patterns* of size 4, have been shown to be in a (size-preserving) bijection with *mosaic* or *diagonal* rectangulations [3] — that is, rectangulations considered up to the weak equivalence. This bijection can be restricted to a bijection between *separable permutations*, defined by avoidance of the patterns 2413 and 3142 [16], and the so-called *guillotine* rectangulations (also known as *sliceable* rectangulations). These results can be fruitfully compared to a basic result in Catalan combinatorics, namely the bijection between *triangulations* of a convex polygon and 231-avoiding permutations [74].

The combinatorics of such families has been analyzed in the framework of *congruences* of the *weak Bruhat order* [65]. The weak Bruhat order is the ordering of the permutations of $[n]$ by inclusion of their set of inversions. A congruence is an equivalence relation on the elements of a lattice that is consistent with the meet and join operations. Catalan families and mosaic rectangulations are both examples of families that define congruences of the weak Bruhat order. As a consequence, the corresponding families (of pattern-avoiding permutations or tessellations) are ordered by a lattice, defined as the *quotient* of the weak Bruhat order by the congruence. It was shown by Pilaud and Santos [62] that the cover graphs of these quotients are all skeletons of polytopes, that they called *quotientopes*. In the case of triangulations and other Catalan objects, the quotient lattice is the well-studied *Tamari lattice* [60] and the quotientope is the ubiquitous *associahedron* [75, 54, 27]. The quotientope of mosaic rectangulations, on the other hand, is known to be a Minkowski sum of two associahedra [53].

In 2012, Reading [66] studied rectangulations considered up to the strong equivalence. He showed that, similarly to the weak case, they are bijective to equivalence classes of permutations that form congruence classes and thus induce a quotient of the weak Bruhat order, and also to so-called *2-clumped permutations*.

Subsequently, Meehan [57] analyzed the cover relation in this quotient, yielding a nice *flip graph* on generic rectangulations. From Pilaud and Santos [62], this flip graph is the skeleton of the quotientope of generic rectangulations.

The main goals that motivated the study presented in this paper were as follows:

1. To develop a uniform treatment of mappings between permutations and rectangulations that would unify the results from earlier contributions and emphasize parallelism and differences between the weak and the strong cases.
2. To simplify the description of the bijection between generic rectangulations and 2-clumped permutations, and give a concise characterization of the corresponding congruence classes of the weak Bruhat order.
3. To find a permutation class in bijection with guillotine generic rectangulations.
4. To address the enumeration of guillotine generic rectangulations. Under the weak equivalence, the generating function of all rectangulations is (non-algebraic) D-finite, while the generating function of guillotine rectangulations is algebraic. Under the strong equivalence, the generating function for all rectangulations is not D-finite, while the status of the generating function for guillotine rectangulations is yet to be determined.

Our results. The first part of our contribution is on the strong equivalence relation and strong rectangulations. We define the *strong order* on rectangles of a strong rectangulation, and prove that the linear extensions of this strong order form equivalence classes of permutations that are bijective with strong rectangulations, and are intervals in the weak Bruhat order. We naturally derive bijections between strong rectangulations and, respectively, 2-clumped and co-2-clumped permutations — the minimum and the maximum of the equivalence classes.

The material in this part streamlines and simplifies a number of previous works. On one hand, Reading [66] (see also Meehan [57] and Merino and Mütze [59]) considers the combinatorics of strong rectangulations and defines the same permutations-to-rectangulations mapping as ours. We present simple incremental algorithms for the forward and backward directions of this mapping that allow for simpler and more direct proofs. In particular, our forward algorithm yields a simple proof for the description of the flip graph studied by Meehan [57]. Our definition of the strong poset for the strong equivalence relation between rectangulations is an analogue of the adjacency poset for weak equivalence defined by

Meehan [56]. Interestingly, it appears that the mapping defined by Reading has already been studied in the form of the "FT-squeeze" algorithm, devised by Fujimaki and Takahashi [46, 77] for VLSI design. The strong poset that we introduce is equivalent to the "seagull order" proposed by Fujimaki and Takahashi as a physical intuition for the FT-squeeze [46]. It also appears in the guise of the elimination process devised by Takahashi, Fujimaki, and Inoue [51, 78] for giving efficient counting and coding methods on strong rectangulations. Finally, our forward algorithm is strongly related to a mapping defined by Françon and Viennot [44] for the analysis of permutations parameterized by their number of peaks, valleys, double ascents, and double descents, and can be analyzed within the framework of quadrant walks. The connection between these numerous lines of work seems to have gone unnoticed so far.

The second part of our paper is dedicated to guillotine rectangulations. We introduce two mesh patterns on permutations that can be used for "encoding" *windmills* — certain configurations of segments, whose occurrence in a rectangulation is equivalent to being non-guillotine. Combining these mesh patterns with the forbidden patterns of Baxter permutations, we obtain new bijections for weak guillotine rectangulations. More interestingly, combining these two mesh patterns with the forbidden patterns for 2-clumped permutations, we obtain a bijection between *strong guillotine rectangulations* (that is, strong equivalence classes of guillotine rectangulations) and a permutation class. This is the first known representation of this family of rectangulations by a permutation class.

The plan of the paper is as follows. In Section 2, we give precise definitions of the objects that we study and review basic results. In particular, the equivalence classes of rectangulations of the weak and strong equivalence will be called, respectively, weak and strong rectangulations. In Section 3, we review earlier results on weak rectangulations: a mapping γ_w from permutations to weak rectangulations, *weak posets* as fibers of this mapping, the induced bijections between weak rectangulations and Baxter, twisted Baxter, and co-twisted Baxter permutations, as well as the structure of the corresponding weak Bruhat order congruence. Then, Section 4 is devoted to an extensive study of the structure of strong rectangulations, while emphasizing its parallelism to the weak case: a mapping γ_s from permutations to strong rectangulations, *strong posets* as fibers of this mapping, and the induced bijections between strong rectangulations and 2-clumped (resp. co-2-clumped) permutations. Moreover, we identify the flip graph on rectangulations, and we show how to encode rectangulations (and subfamilies) by quadrant walks, allowing efficient counting. Finally, in Section 5, we present two mesh patterns p_1, p_2 that "encode" windmills, propose novel permutation classes in bijection with weak and strong guillotine rectangulations, show that the n first terms of the enumerating sequence of strong guillotine rectangulations can be computed in polynomial time in n, and provide lower and upper bounds on the number of strong guillotine rectangulations of size n. The following table shows a summary of bijections between the considered classes of rectangulations and permutation classes, along with the references to the sections where these are discussed.

	Weak equivalence	Strong equivalence
Arbitrary	**Weak rectangulations** Baxter permutations twisted Baxter permutations co-twisted Baxter permutations ⟶ Section 3.4	**Strong rectangulations** 2-clumped permutations co-2-clumped permutations ⟶ Section 4.4
Guillotine	**Weak guillotine rectangulations** separable permutations $\{p_1, p_2\}$-avoiding twisted Baxter perm. $\{p_1, p_2\}$-avoiding co-twisted Baxter perm. ⟶ Sections 2.5 and 5.2	**Strong guillotine rectangulations** $\{p_1, p_2\}$-avoiding 2-clumped permutations $\{p_1, p_2\}$-avoiding co-2-clumped permutations ⟶ Section 5.2

2 Definitions and basics

In this section we present basic notions and definitions used in the paper, as well as some "classical" results. In this exposition, we mainly follow the works by Ackerman, Barequet, and Pinter [3], Law and

Reading [53], Reading [66], Cardinal, Sacristán, and Silveira [26], and Merino and Mütze [59], with some minor modifications for the sake of uniformity.

2.1 Rectangulations and their elements

Let R be an axes-aligned rectangle in the plane. A *rectangulation* of R is a decomposition (or tiling) of R into finitely many interior-disjoint *rectangles*. The *size* of a rectangulation is the number of rectangles in the decomposition. The rectangulation in Figure 1 is of size 13. Rectangulations will generically be denoted by $\mathcal{R}$, and their size by n.

A *segment* of a rectangulation is a maximal straight line segment that consists of one or several sides of some rectangles of $\mathcal{R}$, and is not included in one of the sides of R. A rectangulation is *generic* if there is no point at which four rectangles meet. **From now on, we assume that all rectangulations in this paper are generic. Thus, intersection of two segments of a rectangulation can form a joint of one of the following shapes: $\perp$, $\vdash$, $\top$, $\dashv$, but never $+$.** It is easily shown that a rectangulation of size n has precisely $n-1$ segments. The *neighbors* of a segment s are the segments (perpendicular to s) with an endpoint that lies on s.[1]

We also label the corners of R, or of any rectangle of $\mathcal{R}$, by the ordinal directions: NE for top-right, SE for bottom-right, SW for bottom-left, NW for top-left.

2.2 Weak equivalence and strong equivalence

In order to deal with rectangulations as combinatorial objects, one has to consider some equivalence relation, formalizing the idea of rectangulations "having the same structure". There are two natural ways to do this: the *weak equivalence* that preserves segment–rectangle incidences and sidedness, and the *strong equivalence* that additionally preserves rectangle–rectangle adjacencies.

To give precise definitions, we introduce *left–right* and *above–below* order relations between rectangles of a rectangulation:

- Rectangle r is *on the left* of rectangle r' (equivalently, r' is *on the right* of r) if there is a sequence of rectangles, $r = r_1, r_2, \ldots, r_k = r'$ such that the right side of r_i and the left side of r_{i+1} lie in the same segment for $i = 1, 2, \ldots, k-1$.
- Rectangle r is *below* rectangle r' (equivalently, r' is *above* r) if there is a sequence of rectangles, $r = r_1, r_2, \ldots, r_k = r'$ such that the upper side of r_i and the bottom side of r_{i+1} lie in the same segment for $i = 1, 2, \ldots, k-1$.

Given a rectangle r of $\mathcal{R}$, one can specify the regions that contain the rectangles which are above, below, on the left, or on the right of r, as follows. The *NE alternating path associated with* r is the path that starts at the NE (top-right) corner of r, goes first upwards if the NE corner of r has the shape $\dashv$ or rightwards if it has the shape $\top$, and then alternatingly traverses vertical segments upwards to their upper endpoint then turning rightwards, and horizontal segments rightwards to their right endpoint and then turning upwards, until it reaches the NE corner of $\mathcal{R}$. The NE alternating path associated with r is shown by red in Figure 2. One similarly defines SE, SW, and NW alternating paths. The four alternating paths split $R \setminus \{r\}$ into four regions (some of them can be empty). This leads to the following observation.

Observation 1. *Let r be a rectangle in a rectangulation $\mathcal{R}$.*

1. *The rectangles of $\mathcal{R}$ which lie above, below, on the left, or on the right of r are contained in respective regions of $R \setminus \{r\}$ delimited by the alternating paths (refer to Figure 2).*
2. *Every pair of distinct rectangles in a rectangulation is comparable with precisely one of the order relations: either one of them is on the left of the other, or one of them is above the other.*

Now the two kinds of equivalence of rectangulations are defined as follows.

- Two rectangulations $\mathcal{R}_1$ and $\mathcal{R}_2$ are *weakly equivalent* if there is a (unique) bijection between their rectangles that preserves the left-right and the above-below orders.

[1] In some papers rectangulations are referred to as *floorplans*, their rectangles as *rooms*, and segments as *walls*.

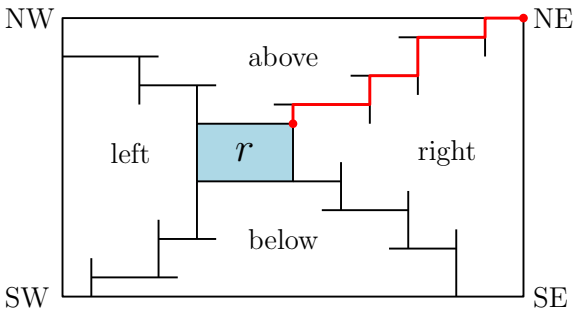

Figure 2: Illustration to Observation 1: four regions delimited by alternating paths.

- Two rectangulations $\mathcal{R}_1$ and $\mathcal{R}_2$ are *strongly equivalent* if they are weakly equivalent, and the bijection that realizes the weak equivalence also preserves adjacencies between rectangles, that is, two rectangles in $\mathcal{R}_1$ are adjacent if and only if the corresponding rectangles in $\mathcal{R}_2$ are adjacent.

These equivalence relations can be also described in terms of local modifications of rectangulations. Two rectangulations are weakly equivalent if they can be obtained from each other by a sequence of moves, where each move is shifting some segment (or one of the sides of R) horizontally or vertically, and accordingly extending or shortening its neighbors, so that the adjacencies between segments do not change. To obtain strong equivalence, we restrict the moves so that the adjacencies between rectangles are also preserved.

A *weak rectangulation* is an equivalence class of rectangulations with respect to the weak equivalence, and a *strong rectangulation* is an equivalence class of rectangulations with respect to the strong equivalence.[2] In Figure 3, rectangulations $\mathcal{R}_1$, $\mathcal{R}_2$, and $\mathcal{R}_3$ are weakly equivalent, but only $\mathcal{R}_1$ and $\mathcal{R}_2$ are strongly equivalent. In other words, here we have two weak rectangulations (one of them is given by three representatives: $\mathcal{R}_1$, $\mathcal{R}_2$, and $\mathcal{R}_3$), and three strong rectangulations (one of them is given by two representatives: $\mathcal{R}_1$ and $\mathcal{R}_2$). **Rectangulation $\mathcal{R}_1$ will be used throughout the paper as a "running example" for demonstrating various results.**

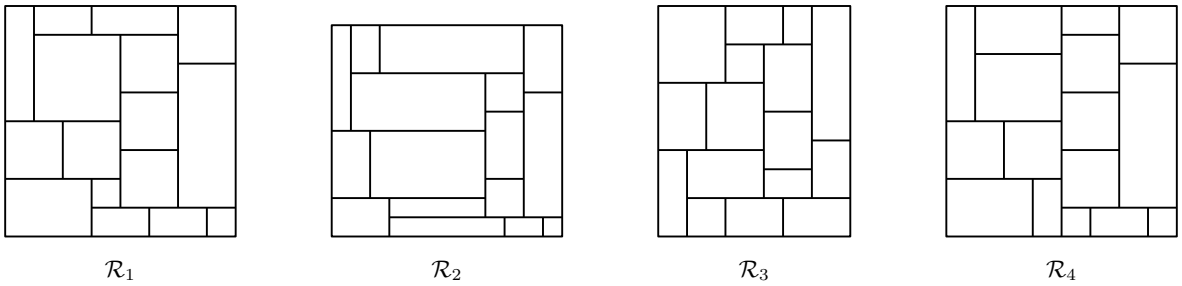

Figure 3: $\mathcal{R}_1$, $\mathcal{R}_2$, and $\mathcal{R}_3$ are weakly equivalent. $\mathcal{R}_1$ and $\mathcal{R}_2$ are strongly equivalent. $\mathcal{R}_4$ is guillotine.

The strong equivalence refines the weak one, and thus every weak rectangulation yields one or several strong rectangulations by all possible *shuffles* of the neighbors of its segments. If a segment s has a neighbors on one side and b neighbors on the other side, then these can be shuffled in $\binom{a+b}{a}$ ways.

2.3 NW–SE and SW–NE labelings

Let $\mathcal{R}$ be a rectangulation. Since, by Observation 1, the transitive relations "left" and "above" yield a partition of the edges of the complete graph, their union "left of, or above" is a total order of the rectangles.

[2] In some earlier papers, for example [66, 59], weak rectangulations are called *mosaic rectangulations*, and strong rectangulations are referred to just as *generic rectangulations*. In [46, 77], weak rectangulations are called *room-to-wall floorplans*, and strong rectangulations are called *room-to-room floorplans*.

Hence, we can label the rectangles by the numbers from 1 to n according to this order. The rectangle with label j ($1 \le j \le n$) will be denoted by r_j. Since r_1 contains the NW (top-left) corner of R and r_n contains the SE (bottom-right) corner of R, we call this labeling *the NW–SE labeling*. If j is fixed, then r_i with $i < j$ are precisely the rectangles above or to the left of r_j, and r_i with $i > j$ are precisely the rectangles below or to the right of r_j: see Figure 4 for a schematic depiction.

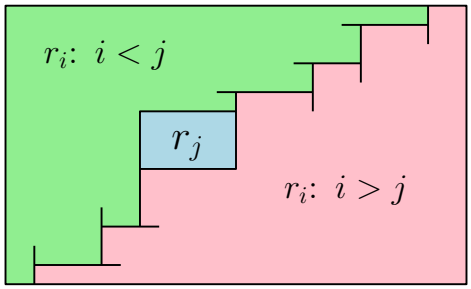

Figure 4: The rectangles r_i with $i > j$ (respectively $i < j$) are located to the right or below r_j (respectively to the left or above r_j).

The NW–SE labeling can also be obtained by the following algorithm.

Algorithm: NW–SE labeling
Input: Rectangulation $\mathcal{R}$.
Output: The NW–SE labeling of the rectangles of $\mathcal{R}$.

1. Label r_1 the rectangle that contains the top-left corner of R.
2. For $j = 2$ to n:

   Consider the joint of segments at the bottom-right corner of r_{j-1}.
   - If its shape is $\dashv$, then label r_j the leftmost rectangle whose upper side belongs to the same horizontal segment as the bottom side of r_{j-1},
   - If its shape is $\perp$, then label r_j the topmost rectangle whose left side belongs to the same vertical segment as the right side of r_{j-1}.

Similarly, one can define the *SW–NE labeling* in which $i < j$ if and only if r_i is to the left or below r_j. It can be obtained by an obvious modification of the algorithm given above. Figure 5 shows the rectangulation $\mathcal{R}_1$ with the NW–SE (left) and the SW–NE (right) labelings of its rectangles. (In this and other examples below, we label the rectangles just j instead of r_j).

2.4 Diagonal rectangulations

A *diagonal rectangulation* of size n is a rectangulation $\mathcal{D}$ of size n, drawn on an $n \times n$ grid square S, such that all the segments are drawn along grid lines, and every rectangle of $\mathcal{D}$ intersects the NW–SE diagonal of S. Diagonal rectangulations have the following properties (see for example [53, Section 5]).

Proposition 2. *(a) Every rectangulation $\mathcal{R}$ is weakly equivalent to a* unique *diagonal rectangulation $\mathcal{D}$, which will be referred to as the* diagonal representative *of $\mathcal{R}$.*

(b) In a diagonal rectangulation we have the following. For every horizontal segment s, all the above neighbors of s occur from the left of all its below neighbors; and for every vertical segment t, all the left neighbors of t occur above all its right neighbors.

(c) The order in which the NW–SE diagonal of S meets the rectangles of a diagonal rectangulation, is the NW–SE order.

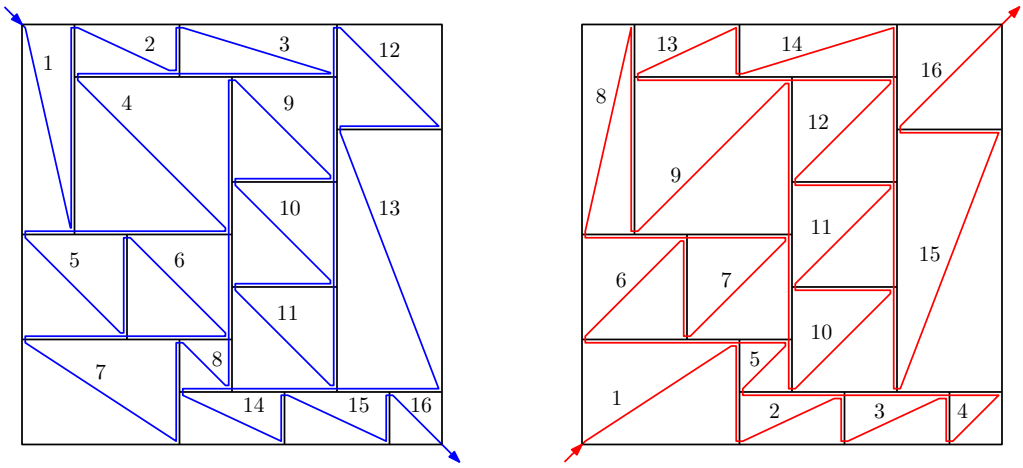

Figure 5: The NW–SE (left) and the SW–NE (right) orderings of the rectangles of $\mathcal{R}_1$.

Due to property (a), diagonal rectangulations are frequently considered as canonical representatives of weak rectangulations (or sometimes even identified with them). Property (b) specifies the unique shuffling of the segments of $\mathcal{R}$ that its diagonal representative can have. In other words, it specifies the unique strong rectangulation which is weakly equivalent to the given $\mathcal{R}$ and strongly equivalent to the diagonal representative of $\mathcal{R}$. Due to property (c), the NW–SE labeling of a diagonal rectangulation is also called *the diagonal labeling*.

One similarly defines *anti-diagonal rectangulations* all of whose rectangles meet the SW–NE diagonal (in the order determined by the SW–NE labeling). In Figure 6 we show the diagonal rectangulation $\mathcal{D}_1$ weakly equivalent to $\mathcal{R}_1$ along with its NW–SE labeling, and the anti-diagonal rectangulation $\mathcal{D}'_1$ weakly equivalent to $\mathcal{R}_1$ along with its SW–NE labeling.

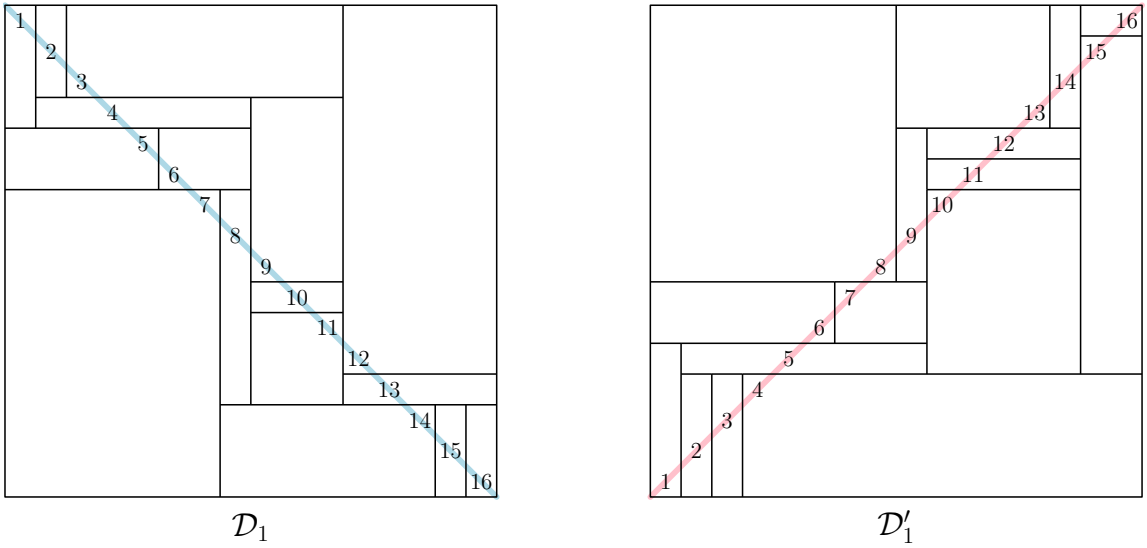

Figure 6: Left: The diagonal rectangulation $\mathcal{D}_1$ weakly equivalent to $\mathcal{R}_1$. Right: The anti-diagonal rectangulation $\mathcal{D}'_1$ weakly equivalent to $\mathcal{R}_1$.

2.5 Guillotine rectangulations

A *cut* of a rectangulation $\mathcal{R}$ is a vertical segment that extends from the top side to the bottom side of R, or a horizontal segment that extends from the left side to the right side of R. If $\mathcal{R}$ has several cuts, then they all have the same orientation.

A rectangulation is *guillotine* if it is either of size 1, or it has a cut s such that both sub-rectangulations separated by s are guillotine. In Figure 3, only rectangulation $\mathcal{R}_4$ is guillotine.

A *windmill* in a rectangulation is a quadruple of segments forming one of the following two shapes: ⊣⊢ or ⊤⊥. (Windmills are also referred to as *pin-wheels* [3].) Note that segments that form a windmill can have arbitrarily positioned further neighbors, also in the *interior* — the rectangular region that they bound. Guillotine rectangulations have the following characterization (proven for instance in [3]).

Proposition 3. *A rectangulation is guillotine if and only if it avoids the windmills* ⊣⊢ *and* ⊤⊥.

The enumeration of weak guillotine rectangulations is nearly elementary. Denote their generating function with respect to the size by $G(x)$. We say that a guillotine rectangulation of size > 1 is *horizontal* or *vertical* in accordance with the orientation of its cut(s). The rectangulation of size 1 is considered neither horizontal nor vertical. Then the generating function of horizontal guillotine rectangulations, and that of vertical guillotine rectangulations, is $H(x) = V(x) = (G(x)-x)/2$. Every vertical guillotine rectangulation is split by its leftmost cut such that the left part is either vertical guillotine or of size 1, and the right part is arbitrary guillotine. This decomposition is unique, and, hence, the generating functions introduced above satisfy the equation

$$V(x) = \big(x + H(x)\big)G(x), \tag{1}$$

which yields

$$H(x) = V(x) = \frac{1 - 3x - \sqrt{1 - 6x + x^2}}{4} = x^2 + 3x^3 + 11x^4 + 45x^5 + \dots,$$

$$G(x) = x + H(x) + V(x) = \frac{1 - x - \sqrt{1 - 6x + x^2}}{2} = x + 2x^2 + 6x^3 + 22x^4 + 90x^5 + \dots. \tag{2}$$

Therefore, we have the following result (proven, for example, in [85] via a bijection to *v-h-trees*, and in [70] via a bijection to *skewed slicing trees*).

Proposition 4. *The number of weak guillotine rectangulations of size n is the $(n-1)$th* Schröder number *(OEIS A006318).*

Multidimensional generalizations of guillotine rectangulations were considered in [4] and [7].

2.6 Permutation patterns

In this section we briefly review the basic definitions and notation from the field of permutation patterns (see also the summary by David Bevan [13]). To specify a permutation, we use the linear notation: that is, $\pi = a_1 a_2 \dots a_n$ is the permutation of $[n]$ that maps i to a_i for $i = 1, 2, \dots, n$. It is convenient to describe such a permutation by a *plot* — the point set $\{(i, a_i)\colon i \in [n]\}$.

Classical patterns. Let $\pi = \pi_1\pi_2\dots\pi_n$ be a permutation of $[n]$, and let τ be a "pattern" — a fixed permutation of $[k]$. An *occurrence* of τ in π is a (not necessarily consecutive) subsequence $\pi_{s_1}\pi_{s_2}\dots\pi_{s_k}$ of π, which is order-isomorphic to τ. If π has an occurrence of τ, we say that π *contains* τ. Otherwise, we say that π *avoids* τ. For example, the permutation $\pi = 32514$ contains the pattern 132 (the subsequence 254 of π is an occurrence of 132); and the permutation $\rho = 43512$ avoids 132.

Vincular patterns. A *vincular pattern* is a pair $v = (\tau, \lambda)$, where τ is a permutation of $[k]$, and λ is a set of one or several pairwise disjoint strings in τ, indicated by underlining (for example $36\underline{185}7\underline{942}$). An occurrence of v in π is an occurrence of τ such that the letters that correspond to the same underlined string occur consecutively in π. For example, the permutation $\pi = 24513$ contains the pattern $2\underline{41}3$ (the subsequence 2513 of π is an occurrence of $2\underline{41}3$); and the permutation $\rho = 25314$ avoids $2\underline{41}3$ (but contains the classical pattern 2413).

Mesh patterns. A *mesh pattern* is a pair $m = (\tau, \mu)$, where τ is permutation of $[k]$, and μ is a subset of $\{0, 1, \dots, k\} \times \{0, 1, \dots, k\}$. An occurrence of m in $\pi \in [n]$ is an occurrence $a_{s_1}a_{s_2}\dots a_{s_k}$ of τ that satisfies

the condition: for every $(i,j) \in \mu$, there is no ℓ such that $s_i < \ell < s_{i+1}$ (with the convention $s_0 = -\infty$ and $s_{k+1} = +\infty$) and $t_j < \pi_\ell < t_{j+1}$, where $t_1 < t_2 < \ldots < t_k$ are the (sorted) elements of $\{a_{s_1} a_{s_2} \ldots a_{s_k}\}$ (with the convention $t_0 = -\infty$ and $t_{k+1} = +\infty$).

To illustrate this concept graphically, we draw the plot of τ and add the grid lines. They split the plane into $(k+1)^2$ regions, which are naturally labeled by $\{(i,j)\colon 0 \le i \le k, 0 \le j \le k\}$. The regions $(i,j) \in \mu$ are then indicated by shading. An occurrence of m in the plot of π is an occurrence of τ such that the interiors of shaded regions do not contain any points of π. See [21] for examples and basic results on mesh patterns. In Section 5, we will work with two mesh patterns, see Figure 26.

If $\tau_1, \tau_2, \ldots, \tau_p$ are some fixed patterns (of any kind), then we denote by $\mathrm{Av}(\tau_1, \tau_2, \ldots, \tau_p)$ the family of permutations that avoid all these patterns. A *permutation class* is any family of permutations that can be specified by avoidance of one or several patterns.

2.7 Permutation classes

In this section we list some permutation classes which will play a role in our paper.

Separable permutations are defined as the class $\mathrm{Av}(2413, 3142)$. Alternatively, they can be defined as permutations that can be recursively constructed from the size-1 permutation by taking direct and skew sums. The equivalence of the two definitions was proven by Ehrenfeucht and Rozenberg [37], and the name "separable permutations" was coined by Bose, Buss, and Lubiw [16]. Separable permutations are enumerated by Schröder numbers, as proven by West [84] via generating trees. For an alternative proof of this fact, note that the definition of weak guillotine rectangulations and the (second) definition of separable permutations yield the same recurrence for their enumerating sequences.

Schröder numbers also enumerate various combinatorial structures, for example *Schröder paths* — the lattice walks from $(0,0)$ to $(2n,0)$ that use steps $(1,1), (2,0), (1,-1)$ and stay (weakly) above the x-axis. Closely related to them are *little Schröder numbers* (OEIS A001003): they were introduced by Ernst Schröder in the context of counting parenthesizations [69]. Remarkably, little Schröder numbers were supposedly mentioned in Plutarch's *Table Talk* (ca. AD 100) in the context of counting compound propositions [73].

The generating function of Schröder numbers is algebraic, it is given above in (2). Singularity analysis readily implies their asymptotics $S_n \sim \frac{(1+\sqrt{2})^{2n+1}}{2^{3/4}\sqrt{\pi n^3}}$ (see [43, note VII.19] and [61, A001003, A006318]).

Baxter permutations are defined as the class $\mathrm{Av}(2\underline{41}3, 3\underline{14}2)$. They were introduced by Baxter and Joichi [9, 10] in the context of commuting real functions.

Baxter permutations are enumerated by *Baxter numbers* (OEIS A001181) given by the explicit formula

$$B_n = \sum_{k=1}^{n} \frac{\binom{n+1}{k-1}\binom{n+1}{k}\binom{n+1}{k+1}}{\binom{n+1}{0}\binom{n+1}{1}\binom{n+1}{2}}.$$

It was first obtained in 1978 by Chung, Graham, Hoggatt, and Kleiman [29]; soon after that Mallows [55] showed that the term corresponding to fixed k is the number of Baxter permutations with precisely $k-1$ descents. Another proof of this formula, via generating trees, was given by Bousquet-Mélou [18]. The generating function of Baxter numbers is D-finite but not algebraic, and their asymptotics is $B_n \sim \frac{2^{3n+5}}{n^4\pi\sqrt{3}}$ [29, "pointed out by A. M. Odlyzko"]. We refer to Felsner, Fusy, Noy, and Orden [41] for a comprehensive survey on combinatorial families enumerated by Baxter numbers and bijections between them.

Twisted Baxter permutations are defined as the class $\mathrm{Av}(2\underline{41}3, 3\underline{41}2)$, and **co-twisted Baxter permutations** as the class $\mathrm{Av}(2\underline{14}3, 3\underline{14}2)$. They are, respectively, the minimum and the maximum of the congruence classes associated to weak rectangulations [53].

Remark. The four patterns $2\underline{41}3, 3\underline{41}2, 2\underline{14}3, 3\underline{14}2$ used in the definition of Baxter, twisted Baxter, and co-twisted Baxter permutations are known as *Baxter-like patterns*. Bouvel, Guerrini, Rechnizter and Rinaldi [19] and Bouvel, Guerrini and Rinaldi [20] investigated the enumeration of permutation families defined by avoidance of all possible combinations of these patterns, by means of generating trees. Five (out of six possible) pairs of Baxter-like patterns yield permutation classes enumerated by Baxter numbers; the exceptional combination is $\{2\underline{14}3, 3\underline{41}2\}$. Permutations that avoid this pair of patterns were studied

by Asinowski, Barequet, Bousquet-Mélou, Mansour, and Pinter [6]: they constitute the "even part" of the so-called "complete Baxter permutations", and they are related to orders between *segments* in rectangulations.

2-clumped permutations are defined by $\mathsf{Av}(24\underline{51}3, 42\underline{51}3, 3\underline{51}24, 3\underline{51}42)$, and **co-2-clumped permutations** are $\mathsf{Av}(24\underline{15}3, 42\underline{15}3, 3\underline{15}24, 3\underline{15}42)$. They are, respectively, the minimum and the maximum of the congruence classes associated to strong rectangulations [66]. The enumerating sequence of these classes is OEIS A342141, and it was proven by Fusy, Narmanli, and Schaeffer [49] that its generating function is not D-finite (via the enumeration of *transversal structures*, which are dual to strong rectangulations).

In Sections 3 and 4, we review and revisit the connection of these classes of permutations with rectangulations, also providing a visual interpretation of the congruence classes associated to weak and strong rectangulations. Specifically, in Theorems 6 and 7, Baxter, twisted Baxter, and co-twisted Baxter permutations will be linked to weak rectangulations, and separable permutations to weak guillotine rectangulations; and, in Theorems 14 and 15, 2-clumped and co-2-clumped permutations will be linked to strong rectangulations.

3 Weak rectangulations

In this section we deal with representation of weak rectangulations by posets and permutations. It has an expository nature and does not contain any new results, therefore we will present the material, mainly from [3, 26, 53, 56], rather briefly and without proofs. We include it in order to provide a systematic summary of all relevant material from different contributions, which makes the comparison with the case of strong rectangulations especially clear and transparent.

As mentioned in Section 2.4, diagonal rectangulations are considered as canonical representatives of weak rectangulations. Therefore, posets and permutations associated with weak rectangulations will be defined via their diagonal representatives.

3.1 The weak poset

We first define the adjacency poset of a rectangulation $\mathcal{R}$. Let the rectangles of $\mathcal{R}$ be labeled with the NW–SE labeling. Then, for two rectangles r_j and r_k of $\mathcal{R}$, we define $j \lhd k$ if r_j and r_k are adjacent, and r_j is on the left of *or* below r_k. In this case we also say that r_j and r_k *block* each other: r_k blocks r_j from the top or from the right, and r_j blocks r_k from the bottom or from the left. The *adjacency poset* $P_a(\mathcal{R})$ is the poset on $[n]$ whose order relation is the transitive closure of $\lhd$.

Now, given a weak rectangulation $\mathcal{R}$, its *weak poset* $P_w(\mathcal{R})$ is defined as the adjacency poset of its diagonal representative $\mathcal{D}$. This poset was introduced by Law and Reading in [53] and thoroughly studied in [56] as a special case of *Baxter posets*.

Note that the adjacency posets of distinct rectangulations weakly equivalent to $\mathcal{R}$ may be different. However, all of them are extensions of the adjacency poset of the corresponding diagonal rectangulation — that is, extensions of $P_w(\mathcal{R})$. Figure 7 shows the rectangulation $\mathcal{R}_1$ and its adjacency poset $P_a(\mathcal{R}_1)$, as well as the diagonal representative $\mathcal{D}_1$ and the weak poset $P_w(\mathcal{R}_1) = P_a(\mathcal{D}_1)$. We draw Hasse diagrams of the weak poset via the natural embedding by duality, and, therefore, the parents of every vertex occur in the increasing order from left to right. This representation also implies that the weak poset $P_w(\mathcal{R})$ is a planar two-dimensional lattice (compare with Proposition 9). Indeed, the planarity is inherited from the $\lhd$-relation which is an orientation of the dual map of $\mathcal{R}$. The cover relations of $P_w(\mathcal{R})$ are a subset of the $\lhd$-relations. The bounded faces of the lattice correspond to segments of $\mathcal{R}$ that have neighbors from both sides.

3.2 Mapping γ_w from permutations to weak rectangulations

Next we describe the fundamental mapping γ_w, introduced by Law and Reading [53], from the set S_n of permutations of size n to the set WR_n of weak rectangulations of size n.

Let $\pi \in S_n$. The corresponding weak rectangulation $\gamma_w(\pi) \in \mathsf{WR}_n$ will be given by its diagonal representative. It is constructed by the following *forward algorithm* that takes an $n \times n$ grid square R and inserts

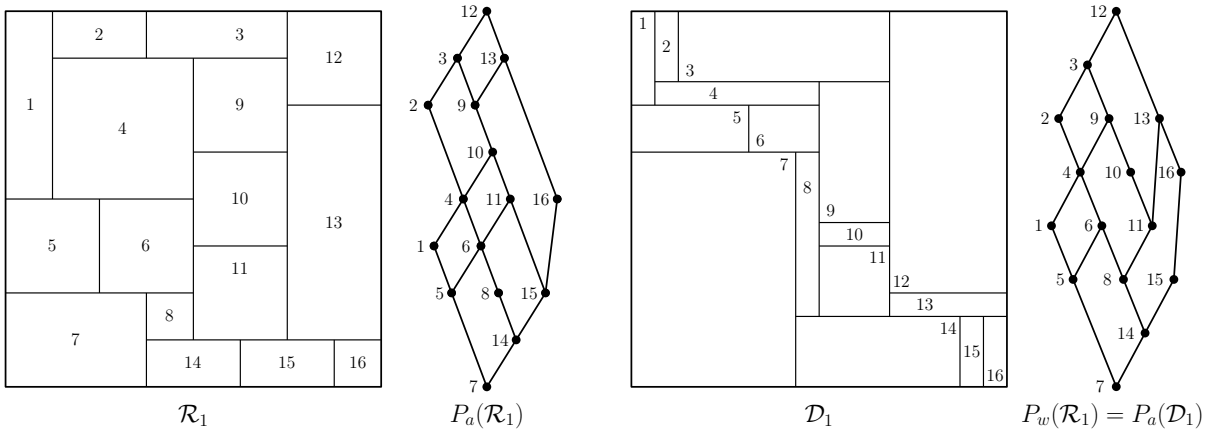

Figure 7: Left: Weak rectangulation $\mathcal{R}_1$ and its adjacency poset $P_a(\mathcal{R}_1)$. Right: The corresponding diagonal rectangulation $\mathcal{D}_1$ and its adjacency poset $P_a(\mathcal{D}_1)$, which is also, by definition, the weak poset $P_w(\mathcal{R}_1)$.

rectangles in the order prescribed by π such that at the end a diagonal rectangulation is obtained. At each step, a *partial rectangulation* — the union of already inserted rectangles — is bounded by a horizontal segment from the bottom, a vertical segment from the left, and a monotonically decreasing *staircase* from the top-right. It is also convenient to adjoin two fictitious rectangles r_0 and r_{n+1} that occupy respectively the column to the left of the grid, and the row below the grid. Accordingly the staircase is extended horizontally at its top-left end, and vertically at its bottom-right end. The turning points of the staircase are referred to as *peaks* $\urcorner$ and *valleys* $\llcorner$. Every peak is labeled according to the rectangle incident to it within the partial rectangulation.

Algorithm WF (weak forward): Permutations to weak rectangulations.
Input: Permutation $\pi = \pi_1\pi_2\dots\pi_n \in S_n$.
Output: Weak rectangulation $\mathcal{R} = \gamma_w(\pi)$.

1. Draw an $n \times n$ square grid R, and label its diagonal cells by $1, 2, \dots, n$ from the top-left to the bottom-right corner. Amend them by an auxiliary rectangle r_0 in the column to the left of the grid, and an auxiliary rectangle r_{n+1} in the row below the grid.
2. Initialize the *staircase* to be the union of the left side and the bottom side of R, extended by a horizontal unit-segment at the beginning, and a vertical unit-segment at the end. Initialize the set of its *peaks* to be $P := \{0, n+1\}$.
3. For i from 1 to n, with $j = \pi_i$:
   Insert rectangle r_j according to the following rules.
   - The bottom-left corner of r_j is the valley delimited by the two consecutive peaks of P with labels a and b such that $a < j < b$.
   - If all rectangles r_k with $a < k < j$ have already been inserted, then the top side of r_j aligns with the top side of r_a. In this case, a is deleted from P. Otherwise, the top side of r_j is contained in the horizontal grid line that separates rows $j-1$ and j.
   - If all rectangles r_k with $j < k < b$ have already been inserted, then the right side of r_j aligns with the right side of r_b. In this case, b is deleted from P. Otherwise, the right side of r_j is contained in the vertical grid line that separates columns j and $j+1$.
   - Update the staircase by replacing the union of left and bottom sides of r_j with the union of its top and right sides. Add j to P.

An example of executing this algorithm is shown in Figure 8.

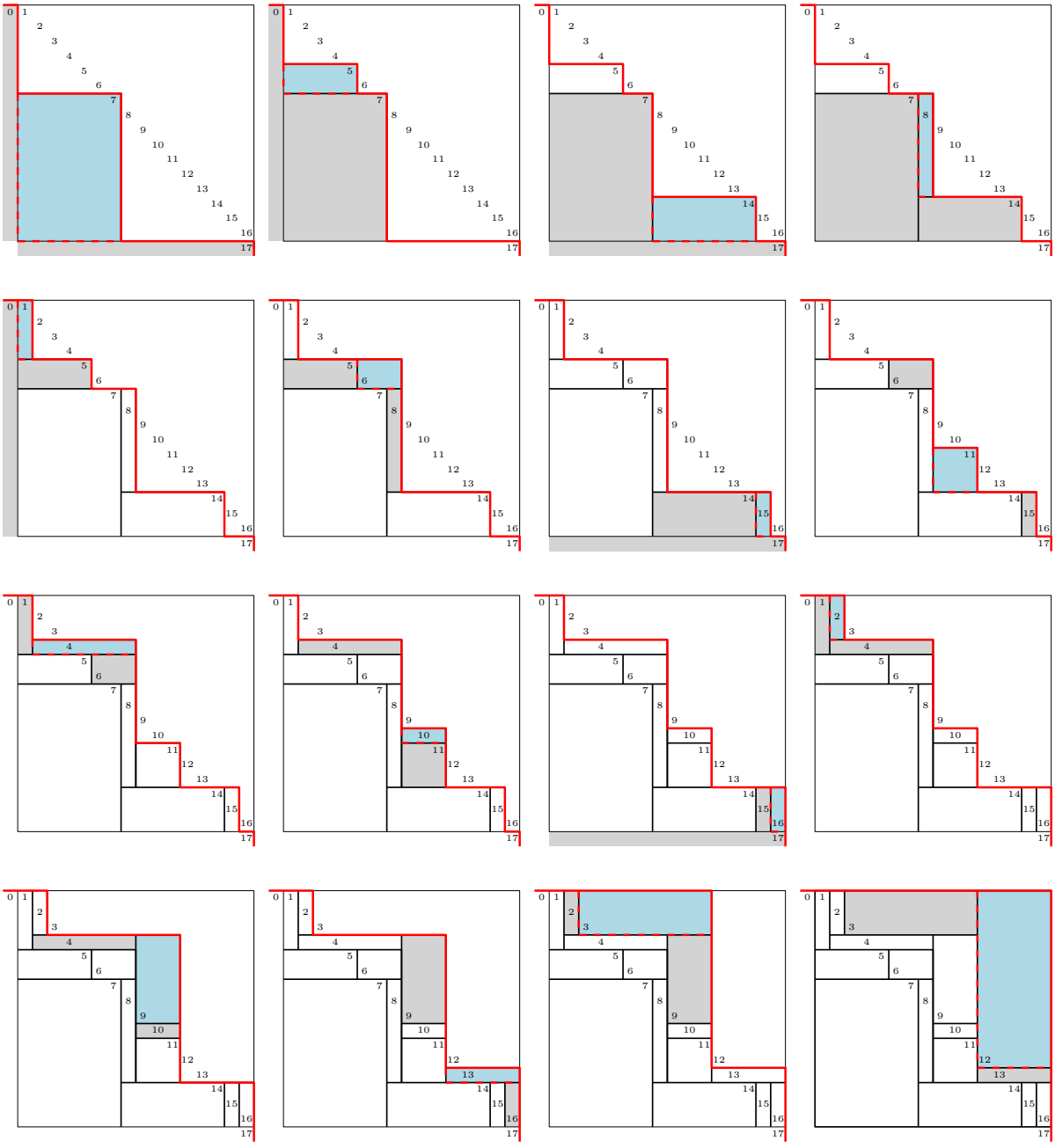

Figure 8: Constructing $\gamma_w(\pi)$ for $\pi = 7\ \ 5\ \ 14\ \ 8\ \ 1\ \ 6\ \ 15\ \ 11\ \ 4\ \ 10\ \ 16\ \ 2\ \ 9\ \ 13\ \ 3\ \ 12$. At each step, the inserted rectangle is blue, and the rectangles incident to the adjacent peaks are grey.

3.3 Fibers

The mapping γ_w is surjective but not injective. Given a weak rectangulation $\mathcal{R}$ of size n, one can recover all permutations $\pi \in S_n$ such that $\gamma_w(\pi) = \mathcal{R}$ by applying the following *backward algorithm* which in fact reverses Algorithm WF. Here, a rectangle r_j of a partial rectangulation $\tilde{R}$ is *available* if it is not blocked from top or from right by some other rectangle of $\tilde{R}$ — that is, if there is no rectangle r_k of $\tilde{R}$ such that $j \lhd k$.

Algorithm WB (weak backward): Weak rectangulations to permutations.
Input: Weak rectangulation $\mathcal{R} \in \mathsf{WR}_n$.
Output: A permutation $\pi \in S_n$ such that $\pi \in \gamma_w^{-1}(\mathcal{R})$.

1. Consider $\mathcal{D}$, the diagonal representative $\mathcal{R}$.
2. Label the rectangles of $\mathcal{D}$ by the NW–SE labeling.
3. For i from n to 1:
   Remove an available rectangle r_j. Set $\pi_i = j$.

Given a poset P, denote the set of its linear extensions by $\mathcal{L}(P)$. The following results are shown in [53, Section 6].

Proposition 5. *Let $\mathcal{R}$ be a weak rectangulation.*

1. *At every step of Algorithm WB there is at least one available rectangle.*
2. *The set of permutations that can be generated by Algorithm WB is precisely the fiber $\gamma_w^{-1}(\mathcal{R})$.*
3. *It is also the set of linear extensions of the weak poset of $\mathcal{R}$:*

$$\gamma_w^{-1}(\mathcal{R}) = \mathcal{L}(P_w(\mathcal{R})).$$

Figure 8, read backwards, demonstrates how π is obtained by Algorithm WB as one of the preimages of $\mathcal{D}_1$. According to Proposition 5, the permutations that can be obtained in this way are precisely the linear extensions of the poset $P_w(\mathcal{R})$ from Figure 7.

Finally, we remark that both algorithms can be performed from the opposite corner: in the forward algorithm one can start inserting rectangles from the top-right corner, and in the backward algorithm one can start removing rectangles from the bottom-left corner, with obvious adjustments of the rules. In both cases, the modified algorithms lead to the same results.

3.4 Baxter, twisted Baxter, and co-twisted Baxter permutations

By Proposition 5, there is a bijection between WR_n and a family of posets on $[n]$, and the linear extensions of all these posets cover the entire S_n. Then we have Theorem 6 concerning distinguished elements of $\mathcal{L}(P_w(\mathcal{R}))$, and Theorem 7 concerning bijective restrictions of γ_w to some permutation classes mentioned in Section 2.7. These results were proven in several contributions, including [3, 26, 53, 56].

Theorem 6. *Let $\mathcal{R}$ be a weak rectangulation, with its rectangles labeled by the NW–SE labeling. Then:*

1. *$\mathcal{L}(P_w(\mathcal{R}))$ contains a unique twisted Baxter permutation. It is the minimum element of $\mathcal{L}(P_w(\mathcal{R}))$ with respect to the weak Bruhat order.*
2. *$\mathcal{L}(P_w(\mathcal{R}))$ contains a unique co-twisted Baxter permutation. It is the maximum element of $\mathcal{L}(P_w(\mathcal{R}))$ with respect to the weak Bruhat order.*
3. *$\mathcal{L}(P_w(\mathcal{R}))$ contains a unique Baxter permutation. It is obtained by reading the labels of the rectangles of $\mathcal{R}$ in the SW–NE (anti-diagonal) order.*

Theorem 7. *The mapping γ_w restricts to three bijections between weak rectangulations and permutation classes:*

1. *A bijection β_{TB} between weak rectangulations and twisted Baxter permutations;*

2. *A bijection β_{CTB} between weak rectangulations and co-twisted Baxter permutations;*

3. *A bijection β_{B} between weak rectangulations and Baxter permutations.*

Moreover, the bijection β_{B} restricts to a bijection β_{S} between weak guillotine rectangulations and separable permutations.

Note that, given Proposition 5, the three items of Theorem 6 imply the corresponding items of Theorem 7. Hence we only have to care of Theorem 6. Since $P_w(\mathcal{R})$ forms an interval in the weak Bruhat order, the minimum (respectively maximum) of this interval can be obtained by iteratively choosing and deleting the leaf with the smallest (respectively largest) label. Since the leaves (current minima) have increasing labels from left to right in the "embedded" Hasse diagram of $P_w(\mathcal{R})$, this corresponds to pruning the leftmost (respectively rightmost) leaf at every step. Hence, we also refer to the minimum and the maximum elements of $\mathcal{L}(P_w(\mathcal{R}))$, with respect to the weak Bruhat order, as the *leftmost* and the *rightmost* linear extensions of $P_w(\mathcal{R})$. We will denote them by π_L and π_R. Then Theorem 6(1,2) says that the twisted Baxter and the co-twisted Baxter representatives of $P_w(\mathcal{R})$ are precisely π_L and π_R. These two linear extensions are a realizer of the 2-dimensional poset $P_w(\mathcal{R})$, which (as mentioned in Section 3.1) is a planar lattice. Figure 9 shows the twisted Baxter, co-twisted Baxter, and Baxter representatives of $P_w(\mathcal{R}_1)$.

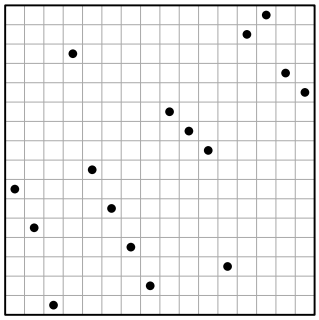

twisted Baxter:
7 5 1 14 8 6 4 2 11 10 9 3 15 16 13 12

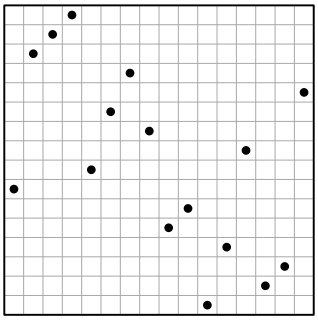

co-twisted Baxter:
7 14 15 16 8 11 13 10 5 6 1 4 9 2 3 12

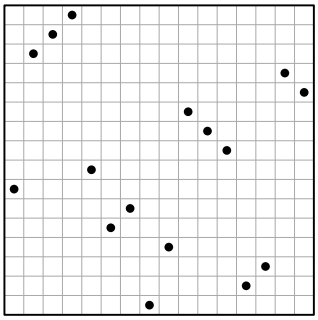

Baxter:
7 14 15 16 8 5 6 1 4 11 10 9 2 3 13 12

Figure 9: The twisted Baxter, co-twisted Baxter, and Baxter representatives of $P_w(\mathcal{R}_1)$.

4 Strong rectangulations

In this section, we consider strong rectangulations. The set of strong rectangulations of size n will be denoted by SR_n. We first discuss their representation by posets and permutations, similarly to the weak case. We define the strong poset of a rectangulation, $P_s(\mathcal{R})$, and a surjective mapping γ_s from S_n to SR_n. The fibers of this mapping define equivalence classes of permutations, which are exactly the linear extensions of the strong poset. In these fibers, we identify two particular representatives — 2-clumped and co-2-clumped permutations, both in bijection with strong rectangulations. This part includes an alternative treatment of results from [66]: in particular, our descriptions of $P_s(\mathcal{R})$ and γ_s lead to a simple geometric proof of the bijections. The new proof makes the correspondence between patterns in rectangulations and patterns in permutations more transparent, additionally, it simplifies the identification of the flip graph of strong rectangulations, and it is well suited to encode strong rectangulations by quadrant walks.

4.1 The strong poset

Let $\mathcal{R}$ be a strong rectangulation of size n. Label the rectangles of $\mathcal{R}$ with their NW–SE labeling. We set $a \blacktriangleleft b$ if one of the following four conditions hold:

1. *adjacency relations* (earlier denoted by $\lhd$ and also called blocking):
   a) r_a and r_b are adjacent, and r_a is on the left of r_b,
   b) r_a and r_b are adjacent, and r_a is below r_b;
2. *special relations* (see Figure 10):
   a) the right side of r_b lies on the same vertical segment as the left side of r_a, and the bottom-right corner of r_b lies above the top-left corner of r_a on this segment,
   b) the top side of r_b lies on the same horizontal segment as the bottom side of r_a, and the top-left corner of r_b lies on the right of the bottom-right corner of r_a on this segment.

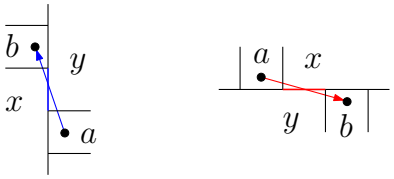

Figure 10: The special relations in the definition of the strong poset. In both cases, we have $a \blacktriangleleft b$.

As above, the adjacency poset $P_a(\mathcal{R})$ is the transitive closure of the adjacency relation $\lhd$. Now, let $\prec_s$ be the transitive closure of $\blacktriangleleft$. Note that the special relations 2a and 2b yield an extension of $P_a(\mathcal{R})$.

Proposition 8. *The relation $\prec_s$ is a partial order on $[n]$.*

Proof. To prove that $\prec_s$ is acyclic, we show that there is a linear order λ on the rectangles of $\mathcal{R}$ which respects the relations of $\prec_s$, and such that the union of rectangles in any prefix of λ is a staircase. The order λ is constructed element by element. Consider the staircase formed by the taken elements, and let $b_1, \ldots, b_k$ be the labels of the rectangles of $\mathcal{R}$ whose bottom-left corners correspond to a valley of the staircase, listed in the left-to-right order. Note that the left side of b_1 is contained in the staircase. If r_{b_1} is a minimal non-taken element with respect to $\prec_s$ — that is, there is no other non-taken element a such that $a \prec_s b_1$ — then we select r_{b_1} as the next element for λ: after that, the taken elements still form a staircase. Otherwise, there is an a such that $a \lhd b_1$ or $a \blacktriangleleft b_1$ due to a special relation. If we have $a \lhd b_1$, then the bottom side of r_{b_1} extends beyond the peak that separates the valleys for r_{b_1} and r_{b_2} in the staircase. If $a \blacktriangleleft b_1$ due to a special relation, then the peak that separates the valleys for r_{b_1} and r_{b_2} in the staircase is the bottom-right corner of r_{b_1}. In both cases we see that $b_2 \prec_s b_1$, and the left side of r_{b_2} is contained in the staircase. Iterating, we obtain a maximum length chain $b_\ell \prec_s b_{\ell-1} \prec_s \ldots \prec_s b_2 \prec_s b_1$, and the left sides of all r_{b_j} for $1 \le j \le \ell$ are contained in the staircase. The bottom side of r_{b_ℓ} is contained in the staircase, since otherwise we have $b_{\ell+1} \prec_s b_\ell$. Hence, r_{b_ℓ} is a minimal element which can be added to λ, such that the remaining elements form a staircase. □

We refer to $\prec_s$ as the *strong order*, and refer to the set $[n]$ partially ordered with respect to $\prec_s$ as the *strong poset* $P_s(\mathcal{R}) = ([n], \prec_s)$ of $\mathcal{R}$. In Figure 11 we show how the strong poset $P_s(\mathcal{R}_1)$ is obtained in two steps from the weak poset $P_w(\mathcal{R}_1)$: first, new adjacencies obtained by shuffling yield $P_a(\mathcal{R}_1)$, the adjacency poset of $\mathcal{R}_1$, and then the special relations yield the strong poset $P_s(\mathcal{R}_1)$.

Proposition 9. *The strong poset $P_s(\mathcal{R})$ is a planar two-dimensional lattice.*

Proof. It is known that planar bounded posets are two-dimensional lattices (see for instance Baker, Fishburn, and Roberts [8]). It therefore suffices to prove that $P_s(\mathcal{R})$ is planar. For this, we consider the planar drawing of the adjacency graph of the rectangles of $\mathcal{R}$ obtained by choosing a point in each rectangle and connecting points in adjacent rectangles by an arc that intersect corresponding edges of the rectangulation. When oriented from left to right and from bottom to top, these edges give all arcs that correspond to adjacency conditions 1a and 1b. Next, we remove all the edges implied by transitivity and obtain the diagram of the adjacency poset. It remains to show that the arcs corresponding to the special relations 2a and 2b can be added without creating crossings. For this, we need two observations:

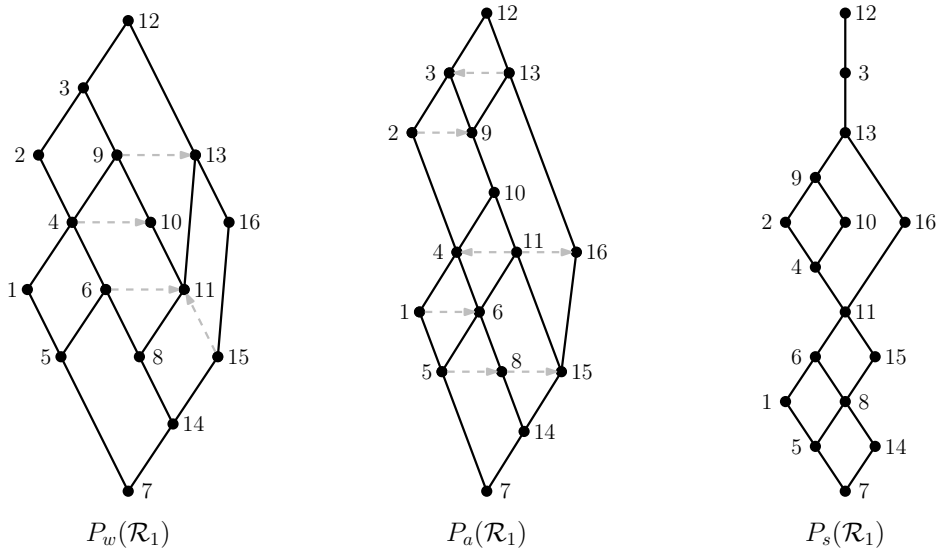

Figure 11: Hasse diagrams of three posets associated with $\mathcal{R}_1$. Left: Solid black edges form $P_w(\mathcal{R}_1)$, the weak poset of $\mathcal{R}_1$ (or: $P_a(\mathcal{D}_1)$ the adjacency poset of $\mathcal{D}_1$); dashed grey edges are new adjacencies contributed by shuffling $\mathcal{D}_1$ into $\mathcal{R}_1$. Middle: Solid black edges form $P_a(\mathcal{R}_1)$, the adjacency poset of $\mathcal{R}_1$; dashed grey edges are contributed by special relations. Right: $P_s(\mathcal{R}_1)$, the strong poset of $\mathcal{R}_1$.

- Every covering special relation is associated with an edge of the rectangulation: a vertical edge that connects the top-left corner of r_a and the bottom-right corner of r_b or a horizontal edge that connects the bottom-right corner of r_a and the top-left corner of r_b (refer to Figure 10). Hence, if we need to draw an arc between two such rectangles r_a and r_b, then these two rectangles are separated by a single edge s.
- The two rectangles r_x and r_y that share edge s are not in the covering relation of the adjacency poset: their adjacency order $x \prec y$ is implied by transitivity. Indeed, referring again to Figure 10, we have either that r_x is below r_b which is left of r_y (special relation 2a), or r_x is above r_b which is right of r_y (special relation 2b). Hence, we can draw the corresponding arc from r_a to r_b without crossing another arc.

These two observations allow us to draw the arcs corresponding to the special relations without creating crossing arcs. Together with the arcs corresponding to the adjacency conditions 1a and 1b, they yield a planar drawing of the Hasse diagram of the strong poset. See Figure 12 for an example. □

4.2 Mapping γ_s from permutations to strong rectangulations

In [66], Reading defined a mapping γ from S_n to SR_n, whose restriction yields a bijection between 2-clumped permutations and strong rectangulations. His construction of $\gamma(\pi)$ consists of two steps: first, one constructs the weak rectangulation corresponding to π — what we denote by $\gamma_w(\pi)$. Then, one shuffles the neighbors of every segment s according to the order in which the labels of rectangles adjacent to s occur in π.

In this section we offer an alternative description of γ (which we denote by γ_s), which consists of just one step and uses a modification of Algorithm WF. Our description emphasizes both the parallelism and the difference between the weak and the strong cases, thus contributing to better understanding of both kinds of equivalence. It also leads to very transparent and descriptive proofs concerning the structure of the strong posets and their linear extensions.

We define the mapping $\gamma_s: S_n \to \mathsf{SR}_n$ via a *forward algorithm* that constructs the rectangulation incrementally: we read the permutation $\pi = \pi_1\pi_2\ldots\pi_n$ from left to right, and insert the rectangle with label $j = \pi_i$ successively, for $i = 1, 2, \ldots, n$. The following invariants hold at every step.

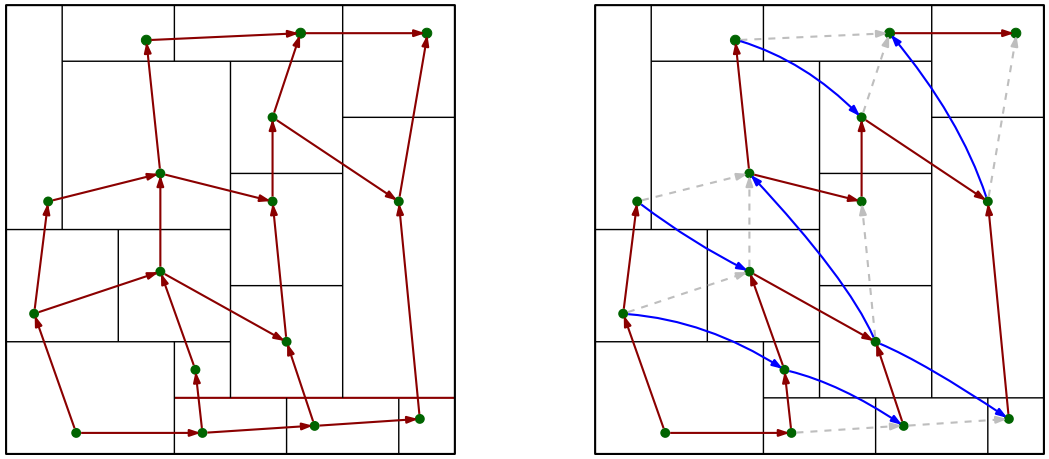

Figure 12: Illustration to the proof of Proposition 9. (a) The Hasse diagram of $P_a(\mathcal{R}_1)$, the adjacency poset of $\mathcal{R}_1$. (b) Solid arcs form the Hasse diagram of $\prec_s$ (the blue arcs are contributed by special relations). The dashed grey arcs belong to $P_a(\mathcal{R}_1)$, but in $P_s(\mathcal{R}_1)$ they are implied by transitivity.

1. The *partial rectangulation* is bounded by a horizontal segment from the bottom, a vertical segment from the left, and a monotonically decreasing *staircase* from the top-right. Similarly to the weak case, we imagine fictitious thin rectangles r_0 and r_{n+1} respectively to the left of the left boundary, and below the bottom boundary, and accordingly we extend the staircase horizontally at its top-left end and vertically at its bottom-right end. We refer to the turning points of the staircase as *peaks* ⌝ and *valleys* ⌞.

2. The labels of the rectangles corresponding to the peaks are in increasing order from top-left to bottom-right, with labels of consecutive peaks differing by at least 2.

Algorithm SF (strong forward): Permutations to strong rectangulations.
Input: Permutation $\pi = \pi_1\pi_2\dots\pi_n \in S_n$.
Output: Strong rectangulation $\mathcal{R} = \gamma_s(\pi)$.

1. Initialize the *staircase* to be made of two peaks, of labels 0 and $n+1$, and one valley. The set P of peaks is thus $\{0, n+1\}$ initially.

2. For i from 1 to n, with $j = \pi_i$:

   Insert rectangle r_j according to the following rules.

   - The bottom-left corner of r_j is the valley delimited by the two consecutive peaks of P with labels a and b such that $a < j < b$.
   - If all rectangles r_k with $a < k < j$ have already been inserted, then the top side of r_j aligns with the top side of r_a, and a is removed from P. Otherwise, the top side of r_j forms a ⊢ with the right side of r_a.
   - If all rectangles r_k with $j < k < b$ have already been inserted, then the right side of r_j aligns with the right side of r_b, and b is removed from P. Otherwise, the right side of r_j forms a ⊥ with the top side of r_b.
   - Update the staircase by replacing the union of left and bottom sides of r_j with the union of its top and right sides. Add j to P.

It is straightforward to verify that the algorithm maintains the invariants above, that it produces a rectangulation, and that the labeling of the rectangles is the NW–SE labeling. Algorithm SF is schematically

illustrated in Figure 13, and an example of its execution for a permutation of size $n = 16$ is given in Figure 14. The four cases of placements in the Algorithm correspond to the four cases considered by Takahashi, Fujimaki, and Inoue [78] in their encoding procedure, and by Françon and Viennot [44] in the proof of their Theorem 2.2 (the current valleys of the partial rectangulation correspond to the current gaps in their iterative encoding of π^{-1}).

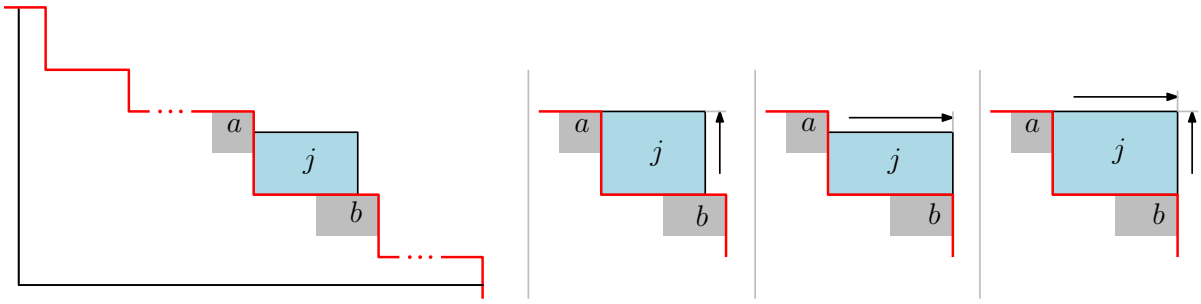

Figure 13: Illustration of the four cases in Algorithm SF. The rectangle with label j is inserted between the peaks of labels a and b such that $a < j < b$. The top (right) sides of r_j are extended, respectively, upwards (to the right) to align with r_a (with r_b) if all rectangles with intermediate labels have already been inserted.

4.3 Fibers

Given a strong rectangulation $\mathcal{R}$ of size n, we now describe a method to recover any permutation $\pi \in S_n$ such that $\gamma_s(\pi) = \mathcal{R}$. This method iteratively removes rectangles, starting from the top right rectangle, and ending with the bottom left rectangle, and constructs a permutation π "from right to left". As in Algorithm WB, we first label the rectangles of $\mathcal{R}$ by the NW–SE labeling. However, in this case the definition of available rectangles is slightly more involved. Let $\tilde{\mathcal{R}}$ be the partial rectangulation of the not yet taken rectangles, the choice of rectangles deleted at each step maintaining the property that its top-right boundary is a staircase. Precisely, a rectangle r_ℓ in $\tilde{\mathcal{R}}$ is called *available* if it satisfies the following conditions, where by convention the top-left corner of $\mathcal{R}$ is a $\top$, and the bottom-right corner is a $\dashv$:

- The top side and the right side of r_ℓ are entirely contained in the staircase.
- The top-left corner of r_ℓ has the shape $\top$; or it has the shape $\vdash$, and the rectangle adjacent to this point from left contains the previous peak.
- The bottom-right corner of r_ℓ has the shape $\dashv$; or it has the shape $\perp$, and the rectangle adjacent to this point from bottom contains the next peak.

Algorithm SB (strong backward): Strong rectangulations to permutations.
Input: Strong rectangulation $\mathcal{R} \in \mathsf{SR}_n$.
Output: A permutation $\pi \in S_n$ such that $\pi \in \gamma_s^{-1}(\mathcal{R})$.

1. Label the rectangles of $\mathcal{R}$ by the NW–SE labeling.
2. For i from n to 1:
   Remove any available rectangle r_j, and set $\pi_i = j$.

The next results show the validity of Algorithm SB.

Lemma 10. *The set of permutations that can be constructed by Algorithm SB is exactly* $\gamma_s^{-1}(\mathcal{R})$.

Proof. At every step of the execution of the forward algorithm, the last rectangle that has been inserted is by definition available among the rectangles that have already been inserted. Conversely, an available

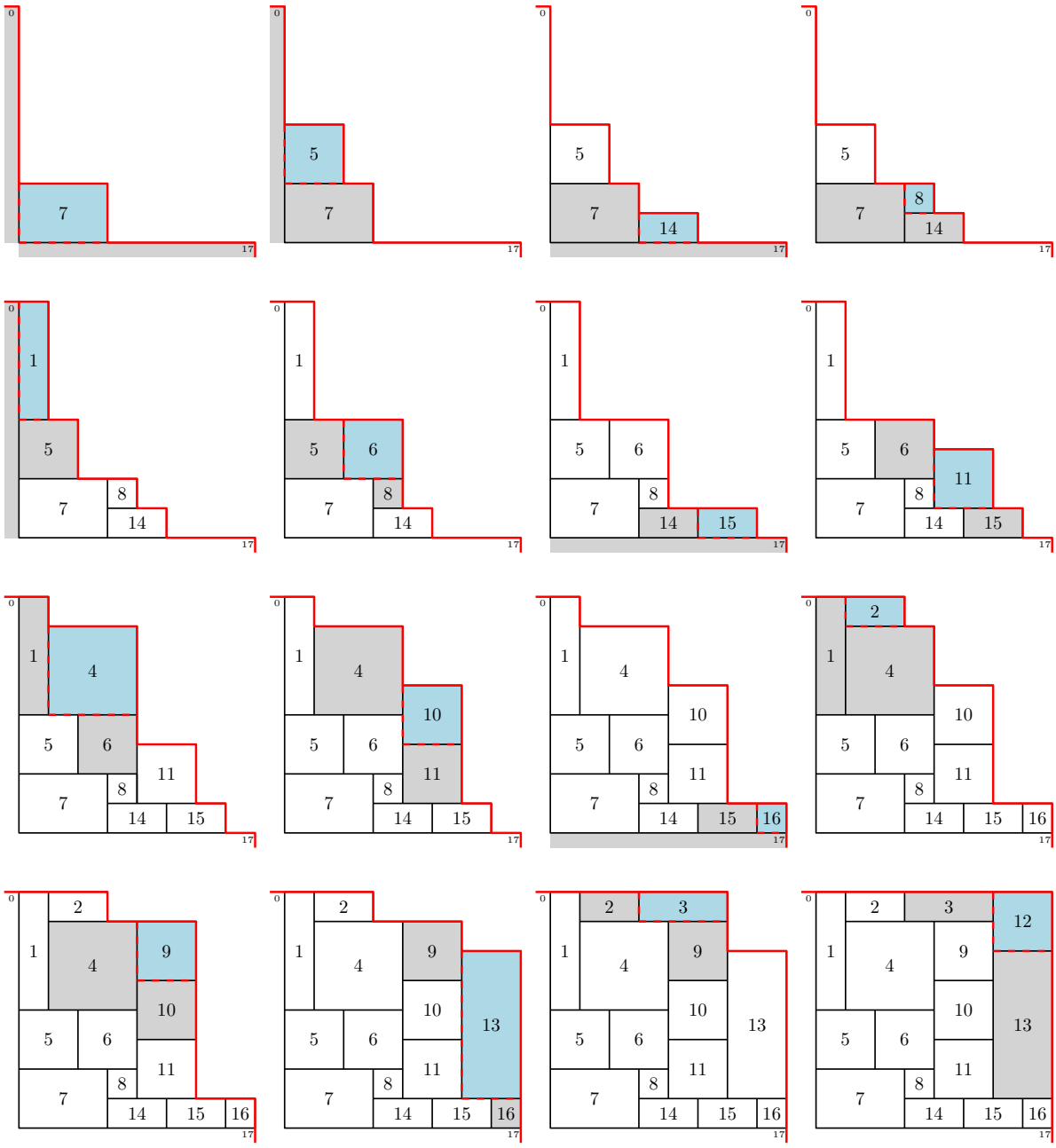

Figure 14: Constructing $\gamma_s(7\ 5\ 14\ 8\ 1\ 6\ 15\ 11\ 4\ 10\ 16\ 2\ 9\ 13\ 3\ 12)$. At each step, the inserted rectangle is blue, and the rectangles incident to the adjacent peaks are grey.

rectangle removed by the backward algorithm is one that could have been inserted by the forward algorithm in the same situation. Hence any execution of the forward algorithm can be mirrored to yield a sequence of rectangles removed by the backward algorithm, and vice versa. □

Then, the following determines precisely how the structure of Algorithms SF and SB is connected with the strong poset. Recall that a subset S of the poset $P_s(\mathcal{R})$ is a *downset* if it is closed for the relation $\prec_s$, hence if $x \in S$ and $y \prec_s x$, then $y \in S$.

Lemma 11. *At every step of Algorithm SB, the set of labels of the remaining rectangles is a downset of $P_s(\mathcal{R})$, and a rectangle r_j is available if and only if j is maximal with respect to $\prec_s$ in that set.*

Proof. We first observe that r_j is available if and only if none of the remaining rectangles r_k satisfies $k \succ_s j$. Indeed, if r_j is available, then the remaining rectangles r_k can touch neither the top nor the right side of r_j, and from the definition of availability, cannot be located as a in the special relations shown in Figure 10. Conversely, if there is no rectangle r_k such that $k \succ_s j$, then r_j is available. Since the backward algorithm removes an available rectangle at each step, the set of remaining rectangles is always a downset of $P_s(\mathcal{R})$. □

Lemma 11 implies the following analogue of Proposition 5.

Proposition 12. *Let $\mathcal{R}$ be a strong rectangulation of size n. Then the fiber $\gamma_s^{-1}(\mathcal{R})$ is exactly the set of linear extensions of $P_s(\mathcal{R})$:*

$$\gamma_s^{-1}(\mathcal{R}) = \mathcal{L}(P_s(\mathcal{R})).$$

Recall that the skeleton graph $\mathcal{G}_n$ of the *permutahedron* is the graph on S_n with edges corresponding to adjacent transpositions. This graph can also be viewed as the cover graph of the weak Bruhat order on S_n. From Proposition 9, we know that $P_s(\mathcal{R})$ is a planar two-dimensional lattice. A realizer of size two of $P_s(\mathcal{R})$ is given by the pair $\{\pi_L, \pi_R\}$ where π_L is the leftmost and π_R is the rightmost linear extension (the definition of the leftmost and the rightmost linear extensions was given in Section 3.4). This implies that the set $\mathcal{L}(P_s(\mathcal{R}))$ of linear extensions is the convex set spanned by π_L and π_R in $\mathcal{G}_n$, i.e., the set of permutations that belong to shortest π_L, π_R paths in $\mathcal{G}_n$ (see for instance Theorem 6.8 in Björner and Wachs [14], or Felsner and Wernisch [42]). Due to the NW–SE labeling of $\mathcal{R}$ we know that if a, b is an incomparable pair then a is left of b in $P_s(\mathcal{R})$ if and only if $a < b$ in the labeling. Hence π_L is the element of $\mathcal{L}(P_s(\mathcal{R}))$ with minimal set of inversions and π_R is the one with maximal set of inversions. This implies the following:

Proposition 13. *Given a strong rectangulation $\mathcal{R}$, the set $\mathcal{L}(P_s(\mathcal{R}))$ of linear extensions of its strong poset induces an interval in the weak Bruhat order on S_n.*

In the next section, we describe the maximum and the minimum of these intervals.

4.4 2-clumped and co-2-clumped permutations

Recall that the class of 2-clumped permutations is defined as $\mathsf{Av}(24\underline{51}3, 42\underline{51}3, 3\underline{51}24, 3\underline{51}42)$, and the class of co-2-clumped permutations is defined as $\mathsf{Av}(24\underline{15}3, 42\underline{15}3, 31\underline{52}4, 31\underline{54}2)$. The following two theorems were proven by Reading in [66].

Theorem 14. *Let $\mathcal{R}$ be a weak rectangulation, with its rectangles labeled by the NW–SE labeling. Then:*

1. *$\mathcal{L}(P_s(\mathcal{R}))$ contains a unique 2-clumped permutation. It is π_L — the minimum (the "leftmost") element of $\mathcal{L}(P_s(\mathcal{R}))$ with respect to the weak Bruhat order.*
2. *$\mathcal{L}(P_s(\mathcal{R}))$ contains a unique co-2-clumped permutation. It is π_R — the maximum (the "rightmost") element of $\mathcal{L}(P_s(\mathcal{R}))$ with respect to the weak Bruhat order.*

Theorem 15. *The mapping γ_s restricts to two bijections between strong rectangulations and permutation classes:*

1. *Bijection β_{2C} between strong rectangulations to 2-clumped permutations;*

2. Bijection β_{C2C} between strong rectangulations to co-2-clumped permutations;

As in the weak case, given Proposition 12, the two items of Theorem 14 imply the corresponding items of Theorem 15. Also similarly to the weak case, one can easily obtain π_L and π_R by repeated pruning the leftmost (respectively, the rightmost) leaf of the Hasse diagram of $P_s(\mathcal{R})$. Figure 15 shows π_L — the 2-clumped representative, and π_R — the co-2-clumped representative of $P_s(\mathcal{R}_1)$.

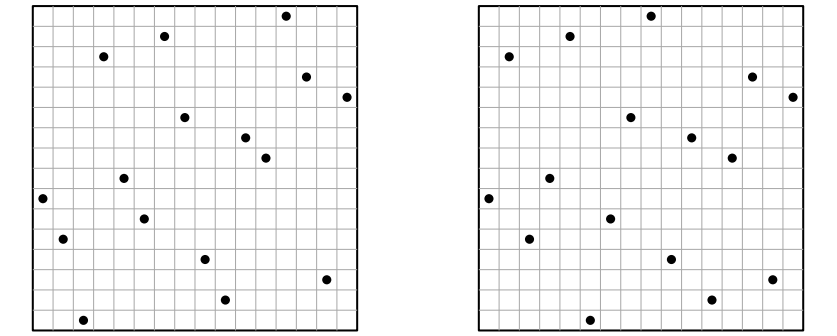

2-clumped:
7 5 1 14 8 6 15 11 4 2 10 9 16 13 3 12

co-2-clumped:
7 14 5 8 15 1 6 11 16 4 10 2 9 13 3 12

Figure 15: The 2-clumped and the co-2-clumped representatives of $P_s(\mathcal{R}_1)$.

Below, we provide an alternative proof of Theorems 14 and 15. Our proof consists of a sequence of lemmas (16, 17, 18), and emphasizes the correspondence between patterns in rectangulations and patterns in permutations. In both cases we prove the part about 2-clumpled permutations; the part about co-2-clumpled permutations then follows by symmetry (Observation 19) — which can also be seen from the characterization of the congruence classes associated to strong rectangulations in [66, Prop 2.2(2)].

Lemma 16. *Let π_L be the leftmost linear extension of $P_s(\mathcal{R})$. Then the pattern $\underline{24}13$ occurs in π_L if and only if the pattern $\dashv$ occurs in $\mathcal{R}$.*

Proof. ($\Rightarrow$) Suppose that the pattern appears in π_L in the form $b\underline{da}c$, where $a < b < c < d$ and d and a appear consecutively. Since π_L is the leftmost linear extension, we necessarily have $d \prec_s a$, otherwise a would occur in π_L earlier than d. Just after taking r_d, the rectangle r_a is available: hence, there is a segment s which contains either the bottom side of r_a and the top side of r_d (a possible configuration is shown in Figure 16(a)), or the right side of r_a and the left side of r_d, in which case the bottom-right corner of r_a is higher then the top-left corner of r_d, as shown in Figure 16(b).

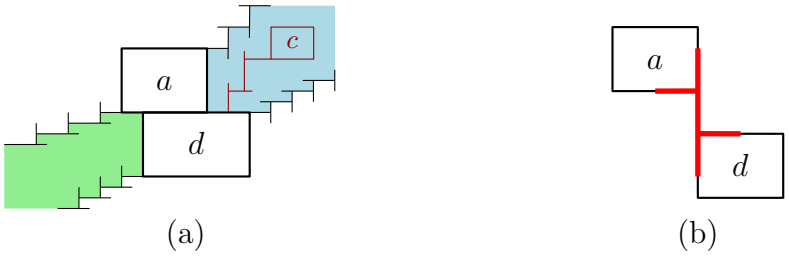

Figure 16: The two possibilities for a covering pair $d \prec_s a$ with $a < d$ in π_L.

If s is horizontal (case (a)), then, by Observation 1(1) (refer also to Figure 4), all the rectangles r_x with $a < x < d$ lie in the union of two regions (shown by green and blue in Figure 16(a)) delimited by the NE and SW alternating paths of r_a and r_d. Since π_L contains the pattern $bdac$, the rectangle r_b lies in the green region, and the rectangle r_c in the blue region. However, considering the SW alternating path of such r_c, we see that the entire green region is below r_c, and, hence, $c < b$, which is a contradiction. Therefore, we necessarily have case (b), and this configuration contains the pattern $\dashv$.

($\Leftarrow$) Suppose that $\mathcal{R}$ contains the pattern $\dashv$. Denote by s the vertical segment, and by r_a and r_d two rectangles contributing to the pattern as in Figure 16 (b). Let b be the lowest rectangle touching s from the left, and c the highest rectangle touching s from the right, see Figure 17(a). We have $a < b < c < d$, and also $c = b + 1$. Then, in any linear extension π of $P_s(\mathcal{R})$, we have the pattern 2413 realized as $bdac$ with $c = b + 1$. It is well known that such a pattern implies an occurrence of $2\underline{41}3$: to see that, note that π has two consecutive letters $d'a'$, with d' weakly on the right of d, and a' weakly on the left of a, such that $d' > c$ and $a' < b$, see Figure 17(b). Then $bd'a'c$ is an occurrence of $2\underline{41}3$. □

Remark. In the proof of ($\Leftarrow$) we did not use the assumption that π_L is the leftmost linear extension. Therefore, in fact, a stronger result holds: If $\mathcal{R}$ contains $\dashv$, then *any* preimage of $\mathcal{R}$ contains $2\underline{41}3$.

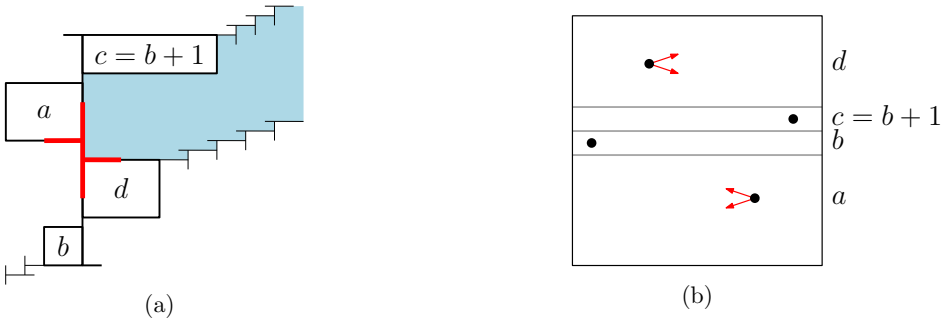

Figure 17: (a) The relative position of the rectangles r_a, r_b, r_{b+1}, r_d in the proofs of Lemmas 16 and 17. (b) An occurrence $bdac$ of 2413, where $c = b + 1$, implies an occurrence of $2\underline{41}3$.

Lemma 17. *The leftmost linear extension π_L of $P_s(\mathcal{R})$ is 2-clumped.*

Proof. Assume for the sake of contradiction that π_L contains one of the four patterns $24\underline{51}3$, $42\underline{51}3$, $3\underline{51}24$, $3\underline{51}42$ forbidden in 2-clumped permutations. Then, clearly, π_L contains $2\underline{41}3$. Then, similarly to the proof of ($\Rightarrow$) in Lemma 16, the pattern $\dashv$ appears in $\mathcal{R}$, realized by four rectangles r_a, r_b, r_c, r_d with labels $a < b < c < d$. Using the argument symmetric to that shown in Figure 17(b), we can assume that $c = b + 1$, and the four rectangles are in the relative position as shown in Figure 17(a).

Consider the possible completions of this occurrence of $2\underline{41}3$ to one of the two patterns $24\underline{51}3$ or $42\underline{51}3$. It follows that there is a rectangle r_x that yields an occurrence of $bx\underline{da}c$ or $xb\underline{da}c$ in π_L, with a, b, c, d fixed as above and $c < x < d$. Then, the condition $c < x < d$ implies that r_x lies in the region (shown by blue) delimited by the rectangles r_c, r_d, the segment s, and the NE alternating paths of r_c and r_d (note that the SW alternating path of r_d is included in that of r_c). However, r_x is inserted earlier than r_d, and must lie below the staircase obtained just before inserting r_d. Since the blue region is above such a staircase, it is not possible to place r_x so that an occurrence of $42\underline{51}3$ or $24\underline{51}3$ will be created. One can show with a symmetric argument that the occurrence of the pattern $2\underline{41}3$ can neither be completed to an occurrence of $3\underline{51}42$ nor $3\underline{51}24$. Therefore, π_L must be a 2-clumped permutation. □

In order to show that the fibers of γ_s, hence the strong rectangulations, are in bijection with 2-clumped permutations, we need to prove that the leftmost linear extension is the unique 2-clumped one.

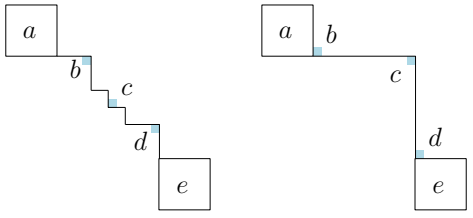

Figure 18: The two cases in the proof of Lemma 18.

Lemma 18. *If a linear extension π of $P_s(\mathcal{R})$ is not the leftmost linear extension, then it is not 2-clumped.*

Proof. Since $\pi \neq \pi_L$, there are two indices i and j with $i < j$ such that π_i and π_j are both minima of the poset induced by $\pi_i, \dots, \pi_n$ and $\pi_j < \pi_i$. By looking at the elements between π_i and π_j we find an index ℓ with $i \leq \ell < j$ such that $\pi_{\ell+1} < \pi_\ell$ and such that π_ℓ and $\pi_{\ell+1}$ are both minima of the poset induced by $\pi_\ell, \dots, \pi_n$.

Let $a = \pi_{\ell+1}$ and $e = \pi_\ell$. Note that a and e are incomparable in $P_s(\mathcal{R})$. Consider the rectangles of $\mathcal{R}$ with labels in the prefix $\pi_1 \dots \pi_{\ell-1}$ of π: They form a staircase such that the rectangles r_a and r_e are in two valleys, the one for r_a before the one for r_e along the staircase. We consider this staircase and distinguish two cases, see Figure 18.

First, if there is a valley between the valleys occupied by r_a and r_e, then the bottom side of r_a and the left side of r_e belong to two segments forming two peaks belonging to two different rectangles r_b and r_d with $a < b < d < e$. Consider the next rectangle r_c to be inserted in a valley between those occupied by r_a and r_e. Due to the NW–SE labeling, we have $b < c < d$, and in π we first have b and d in any order, then consecutively ea, and finally c. This yields an occurrence of one of the two forbidden patterns $24\underline{51}3$ and $42\underline{51}3$.

Now suppose that the rectangles r_a and r_e are inserted in consecutive valleys. Let r_c be the rectangle forming the peak between the valleys of r_a and r_e. We claim that neither r_a nor r_e extend to the top-right corner of r_c. Indeed, if r_e extends to the top-right corner of c, then we have $a \prec_s e$ due to the special relations; and similarly, if r_a extends to the top-right corner of r_c, then $e \prec_s a$. Both are impossible since a and e are incomparable in $P_s(\mathcal{R})$. Hence, adding r_a and r_e to the staircase makes two valleys, one on each side of r_c. Let r_b and r_d be the rectangles filling these valleys. From the order along the staircase we obtain $a < b < c < d < e$, while in π we first have c then consecutively ea, and finally b and d in any order. This yields one of the other forbidden patterns $3\underline{51}24$ and $3\underline{51}42$. □

Lemmas 16, 17 and 18 together imply Theorems 14(1) and 15(1).

Given a permutation π in S_n, its *complement* $\bar{\pi}$ is the permutation whose ith component is $\bar{\pi}_i = n+1-\pi_i$. Note that the forbidden patterns of co-2-clumped permutations are the complements of the forbidden patterns of 2-clumped permutations.

The following fact is a direct consequence of the symmetry of the forward algorithm.

Observation 19. *The rectangulation $\bar{\mathcal{R}} = \gamma_s(\bar{\pi})$ is symmetric to $\mathcal{R} = \gamma_s(\pi)$ with respect to the SW–NE diagonal.*

Since the rightmost linear extension of $P_s(\mathcal{R})$ is the complement of the leftmost linear extension of $P_s(\bar{\mathcal{R}})$, it must forbid the complements of the forbidden patterns for the 2-clumped permutations. Therefore, the rightmost linear extension π_R of $P_s(\mathcal{R})$ is co-2-clumped, and if a linear extension π of $P_s(\mathcal{R})$ is not the rightmost linear extension, then it is not co-2-clumped. Hence co-2-clumped permutations are exactly the maxima, in the weak Bruhat order, of the intervals $\gamma_s^{-1}(\mathcal{R})$, and they are bijective to strong rectangulations as well. This completes the proof of Theorem 14 and 15.

Remark. Combining Theorem 15 with Lemma 16, we observe that γ_s specializes into a bijection from permutations that avoid $2\underline{41}3$ — the *semi-Baxter permutations* — to rectangulations that avoid $\dashv$. By duality [49, Sec.2.4], rectangulations of size n avoiding $\dashv$ are in bijection with plane bipolar posets with $n+2$ vertices, which are in a simple bijection [49, Sec.5] with permutations of size n that avoid $2\underline{14}3$ (*plane permutations*). Plane permutations are shown in [19] to be in bijection with semi-Baxter permutations, but the bijection is recursive (it proceeds via generating trees). Via rectangulations avoiding $\dashv$ we have a more geometric bijection between these two permutation classes.

Moreover, by symmetry, γ_s specializes into a bijection from permutations avoiding $3\underline{14}2$ to rectangulations avoiding $\vdash$. So γ_s specializes into a bijection from Baxter permutations to rectangulations avoiding $\dashv$ and $\vdash$, which identify with weak rectangulations (and are realized by the anti-diagonal representation), and we recover the bijection from [3] between Baxter permutations and weak rectangulations.

4.5 The flip graph on strong rectangulations

We briefly recall the notion of lattice congruence, and refer to Reading [65] for a specific treatment of congruences of the weak Bruhat order. An equivalence relation $\equiv$ on the set of elements of a lattice $(L, \wedge, \vee)$

is said to be a *lattice congruence* if it behaves consistently with respects to joins and meets, hence if $x \equiv x'$ and $y \equiv y'$, then $x \wedge y \equiv x' \wedge y'$, and $x \vee y \equiv x' \vee y'$. In that case, one can define the quotient of the lattice on the congruence classes, such that the order as well as the meet and the join of two classes is defined respectively by the order, the meet, and the join in L of any two representatives of the classes. The lattice quotient can also be shown to be isomorphic to the lattice induced in L by the minimal element of each congruence class. It is known that the equivalence classes of permutations defined by the fibers of γ_s form a lattice congruence.

Theorem 20 (Reading [66])**.** *Consider the equivalence relation $\equiv$ on S_n defined by*

$$\pi \equiv \sigma \Leftrightarrow \gamma_s(\pi) = \gamma_s(\sigma).$$

Then $\equiv$ is a lattice congruence of the weak Bruhat order $\prec$ on S_n.

In particular, the partial order induced by the weak Bruhat order on these equivalence classes is a lattice. The cover graph of this lattice is a graph with vertex set SR_n. Meehan [56] described the edges of this graph as local operations on the rectangulations, so that two rectangulations are adjacent if and only if they differ by such an operation. These operations are called *flips*, and the cover graph of the lattice on SR_n is called the *flip graph* on SR_n. This is in perfect analogy with the well-known flip graph on triangulations of a convex polygon defined by the Sylvester congruence [79], and the flip graph on diagonal rectangulations defined by the Baxter congruence [53]. These flip graphs happen to be skeletons of polytopes: Flip graphs on triangulations, for instance, are skeletons of associahedra [72, 63]. A remarkable result by Pilaud and Santos allow us to make the same statement for the flip graph on strong rectangulations.

Theorem 21 (Pilaud and Santos [62])**.** *For any lattice congruence $\equiv$ of the weak Bruhat order on S_n, the cover graph of the quotient of the weak Bruhat order by $\equiv$ is the skeleton of a polytope.*

Our algorithm describing the mapping γ_s allows us to identify the flip operations defining the graph of this strong rectangulation polytope.

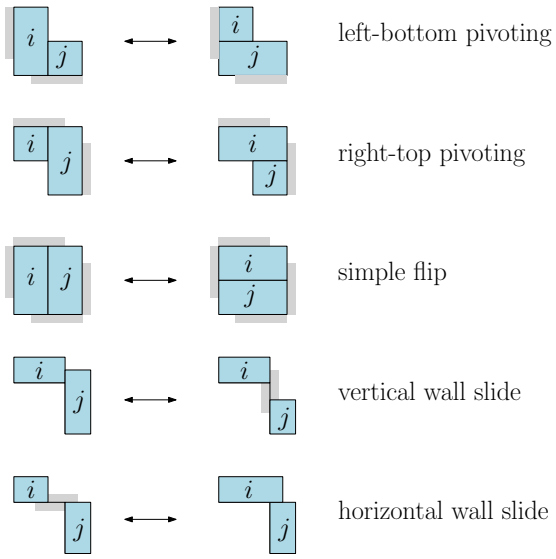

Figure 19: Flips in strong rectangulations that correspond to cover relation in the lattice of strong rectangulations. These are obtained by considering the changes that occur in the rectangulations when the forward algorithm is applied on two permutations that differ by the adjacent transposition of i and j. In all five situations, the shaded regions cannot intersect any edge of the rectangulation, by the definition of the mapping γ_s.

Theorem 22. *The flip graph on the set of strong rectangulations SR_n is described by the flip operations of Figure 19.*

Proof. Observe that if we consider two permutations π and π' differing by one adjacent transposition, then either $\pi \equiv \pi'$ or, by definition of a lattice congruence, $\gamma(\pi)$ and $\gamma(\pi')$ are in a cover relation in the lattice quotient, hence $\gamma(\pi)$ and $\gamma(\pi')$ differ by a flip. It therefore suffices to inspect all changes in the rectangulation $\gamma(\pi)$ that can occur when two adjacent entries of π are transposed.

Recall that the forward algorithm reads the input permutation $\pi = \pi_1\pi_2\dots\pi_n$ from left to right, and at each step t, inserts the rectangle r_{π_t}, with label π_t. Consider two successive steps of the algorithm, involving $\pi_t = i$ and $\pi_{t+1} = j$. Suppose, without loss of generality, that $i < j$. There are five possible ways that the rectangles change placement after the transposition of i and j, which are illustrated in Figure 19. Note that in this figure, the grey regions cannot intersect any edge of the rectangulation. This follows from the way that the rectangles r_i and r_j, as well as any rectangle processed later, are inserted by the forward algorithm. In all five cases, the transformation in $\mathcal{R}$ is of one of three types of flips: pivoting flips, simple flips, and wall slides.

Conversely, if such an operation is possible in a rectangulation $\mathcal{R}$, then there is an execution of the forward algorithm such that the two rectangles involved are inserted consecutively. One can, for instance, consider the downset $S_{i,j} \subset [n]$ of labels ℓ such that either $\ell \prec_s i$, or $\ell \prec_s j$, and consider any linear extension of $(S_{i,j}, \prec_s)$. By Proposition 12, running the forward algorithm on this prefix of a permutation leads to a situation in which we can insert either r_i or r_j, and the flip can be implemented. □

4.6 Quadrant walk encoding and enumeration

From the definition of the forward algorithm, we can now establish bijections between families of strong rectangulations and families of quadrant walks (we also discuss how the method adapts in the weak case).

For a point $p = (x, y)$ in the quadrant $\mathbb{N}^2$, the *level* of p is $h(p) := x + y$. We define a *history quadrant walk* as a sequence of points (x, y) in the quadrant $\mathbb{N}^2$, each point having a color in {black, red, green, white}, such that for any two consecutive points p, p' of the sequence:

- if p is black, then $h(p') = h(p) + 1$,
- if p is red or green, then $h(p') = h(p)$,
- if p is white, then $h(p') = h(p) - 1$.

Such a walk is called *closed* if the final point is at the origin and is white; it is called an *excursion* if it is closed and starts at the origin.

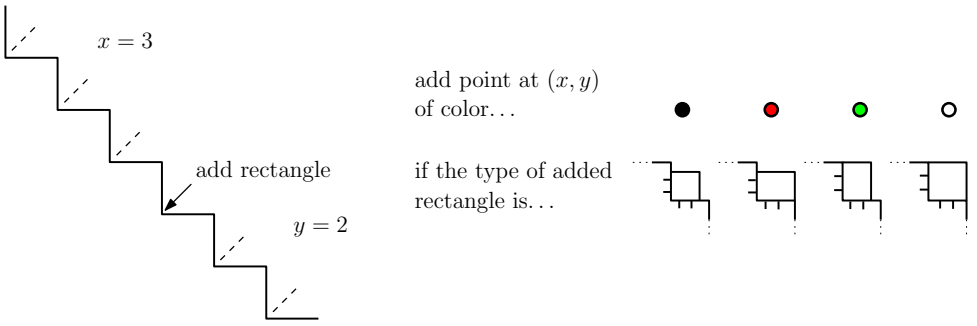

Figure 20: Rule for inserting a colored point in the quadrant, corresponding to inserting a rectangle by the forward algorithm.

For π a permutation of size n, with $\mathcal{R} = \gamma_s(\pi)$ the rectangulation produced from π by the forward algorithm, the corresponding *quadrant history* is the history quadrant excursion (with n points) where each rectangle addition yields a point as shown in Figure 20. See also Figure 21 for a complete example.

Remark. A *bicolored Motzkin excursion* is a Motzkin excursion (walk with steps in $\{(1,1),(1,0),(1,-1)\}$, starting at the origin, staying in $\{y \geq 0\}$, and ending on the line $\{y = 0\}$) where each horizontal step is colored either red or green, it is *decorated* if each point of the excursion is assigned an integer x between 0

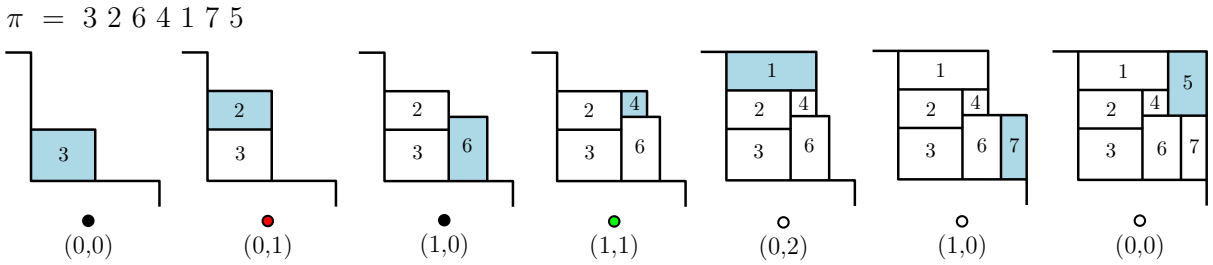

Figure 21: A permutation π, and the associated quadrant history σ, which is built jointly with the rectangulation $\mathcal{R}$ produced by the forward algorithm (note that π is not needed to build $\mathcal{R}$ from σ).

and its height. For π a permutation of size n, the quadrant history σ of $(\pi, \mathcal{R} = \gamma(\pi))$ can be encoded by a decorated bicolored Motzkin excursion (of length $n-1$), where the successive heights in the Motzkin excursion are given by the sequence of levels of points in σ, the horizontal steps are colored as the initial point of the corresponding step in σ, and the assigned integers are given by the abscissas of points in σ. One can check that this decorated bicolored Motzkin excursion is the one associated to the permutation π^{-1} by the Françon-Viennot bijection [44].

A history quadrant walk is called *leftmost* if, for any two consecutive points p, p':

- if the color of p is in {black,red} and the color of p' is in {black,green}, then $x(p') \geq x(p)$,
- otherwise, $x(p') \geq x(p) - 1$.

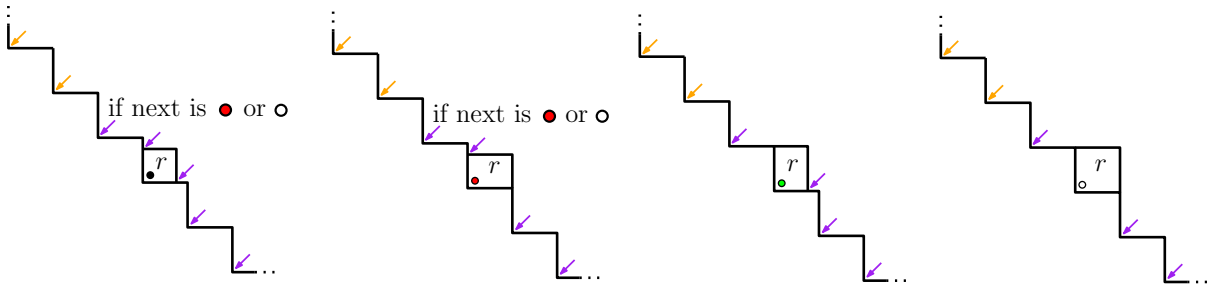

Figure 22: If the last inserted rectangle r is the current rightmost available rectangle, the figure indicates for each valley whether the insertion of a rectangle r' at that valley makes r' the new rightmost available rectangle (purple) or not (orange). As shown, when r is of black or red type, there is a mixed valley to the left of r, where r' is allowed to be inserted only if it is red or white (indeed, in that case, r is not available anymore after inserting r').

As shown in [51] (in different but equivalent terms) and illustrated in Figure 22, the quadrant history of a pair $(\pi, \mathcal{R} = \gamma(\pi))$ is leftmost if and only if π is the leftmost linear extension of $P_s(\mathcal{R})$, that is, at any step, the last added rectangle is the rightmost available rectangle. We therefore obtain the following.

Proposition 23. *Leftmost history quadrant excursions of length $n-1$ (hence having n points) are in bijection with rectangulations of size n, and with 2-clumped permutations of size n.*

The above characterization can be turned into a recurrence for counting these walks, and gives an efficient procedure for counting rectangulations [51] (other polynomial-time counting methods have been given respectively in [30] via inclusion-exclusion, and in [49] by a different quadrant walk encoding, via some decorated plane bipolar orientations). The sequence starts with $1, 2, 6, 24, 116, 642, 3938, 26194, 186042, 1395008, \ldots$ (OEIS A342141). As shown in [49] (and in [45, 78] for the upper bound), its exponential growth rate is $27/2$.

Symmetrically, a history quadrant walk is called *rightmost* if, for any two consecutive points p, p':

- if the color of p is in {black,green} and the color of p' is in {black,red}, then $y(p') \geq y(p)$,
- otherwise, $y(p') \geq y(p) - 1$.

These correspond to pairs $(\pi, \mathcal{R} = \gamma(\pi))$ such that π is the rightmost linear extension of $P_s(\mathcal{R})$ (at any step, the last added rectangle is the leftmost available one), which occurs if and only if π is co-2-clumped.

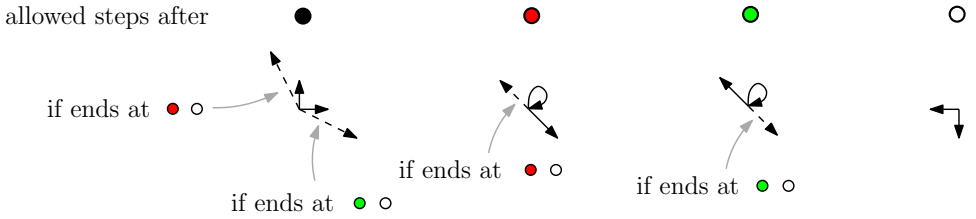

Figure 23: The allowed steps in leftright history walks (special steps are shown dashed).

A history quadrant walk is called *leftright* if it is both leftmost and rightmost. Equivalently, it is a history walk (here better formulated in terms of allowed steps) such that, for any two consecutive points p, p' (see Figure 23):

- If p is black, then from p to p' the steps $(0,1)$ and $(1,0)$ are allowed. Furthermore, if the color of p' is in {red,white} then the step $(-1,2)$ is allowed, and if the color of p' is in {green,white} then the step $(2,-1)$ is allowed, such steps being called special.
- If p is red, then from p to p' the steps $(0,0)$ and $(1,-1)$ are allowed, and furthermore the step $(-1,1)$, called a special step, is allowed if the color of p' is in {red,white}.
- If p is green, then from p to p' the steps $(0,0)$ and $(-1,1)$ are allowed, and furthermore the step $(1,-1)$, called a special step, is allowed if the color of p' is in {green,white}.
- If p is white, then from p to p' the allowed steps are $(-1,0)$ and $(0,-1)$.

Leftright history quadrant excursions thus correspond to rectangulations $\mathcal{R}$ such that $P_s(\mathcal{R})$ is a total order, i.e., the fiber has size 1 (indeed, at any step, the last added rectangle is both the leftmost and rightmost available rectangle, hence is the unique available rectangle), a superfamily of rectangulations avoiding $\dashv$ and $\vdash$ (those represented by anti-diagonal rectangulations). These also correspond to permutations that are 2-clumped and co-2-clumped (and to equivalence classes of size 1 for the congruence in Theorem 20), a superfamily of Baxter permutations.

The above characterization of leftright walks can be turned into a recurrence as follows. For $\mathcal{G}$ a set of history quadrant walks, and for $n \geq 1, i, j \geq 0$, we let $G_{n,i,j}$ be the number of closed walks of length n in $\mathcal{G}$ and starting at (i,j). Then, with $\mathcal{A}$ the set of leftright history quadrant walks, and with $\mathcal{B}$ (resp. $\mathcal{R}, \mathcal{G}, \mathcal{W}$) the subset of those starting at a black (resp. red,green,white) point, a classical decomposition by first-step removal yields, for $n \geq 1$ and $i, j \geq 0$,

$$\begin{cases} B_{n,i,j} &= A_{n-1;i+1,j} + A_{n-1,i,j+1} + R_{n-1,i-1,j+2} + W_{n-1,i-1,j+2} \\ & \quad + G_{n-1,i+2,j-1} + W_{n-1,i+2,j-1} \\ R_{n,i,j} &= A_{n-1,i+1,j-1} + A_{n-1,i,j} + R_{n-1,i-1,j+1} + W_{n-1,i-1,j+1}, \\ G_{n,i,j} &= A_{n-1,i-1,j+1} + A_{n-1,i,j} + G_{n-1,i+1,j-1} + W_{n-1,i+1,j-1}, \\ W_{n,i,j} &= A_{n-1,i-1,j} + A_{n-1,i,j-1}, \\ A_{n,i,j} &= B_{n,i,j} + R_{n,i,j} + G_{n,i,j} + W_{n,i,j}, \end{cases} \tag{3}$$

with boundary conditions $L_{n;i,j} = 0$ for $n \leq 0$ or $i < 0$ or $j < 0$ (for $L \in \{A, B, R, G, W\}$), except for $W_{0,0,0} = A_{0,0,0} = 1$.

Note that, by $\{x, y\}$-symmetry of the walk specification, we have $R_{n,i,j} = G_{n,j,i}$ (and the coefficients $A_{n,i,j}, B_{n,i,j}, W_{n,i,j}$ are symmetric in i and j). The sequence $U_n = A_{n-1,0,0}$ gives

the number of permutations of size n that are 2-clumped and co-2-clumped[3], it starts with $1, 2, 6, 24, 112, 582, 3272, 19550, 122628, 800392, \ldots$, and, to our knowledge, it has not been considered before.

Proposition 24. *The exponential growth rate of U_n is bounded from above by $\Gamma := \frac{1}{2}(9 + \sqrt{113}) \approx 9.815$.*

Proof. Let

$$\mathbb{A} = \begin{pmatrix} 2 & 3 & 3 & 4 \\ 2 & 3 & 2 & 3 \\ 2 & 2 & 3 & 3 \\ 2 & 2 & 2 & 2 \end{pmatrix}$$

and let $\mathbb{I} = (1, 1, 1, 1)$. Then obviously the number of leftright walks of length n (starting at the origin) with no constraint on domain nor on endpoint is equal to $\mathbb{I} \cdot \mathbb{A}^n \cdot \mathbb{I}^T$; and Γ is the spectral radius of $\mathbb{A}$. □

Remark. From the table of initial coefficients, the ratio U_n/U_{n-1} seems to converge to Γ (this is even more visible when applying acceleration of convergence techniques, see e.g. [50, Sec.6]). By similar calculations as [48, Conjecture 25] (details omitted), letting $\xi = (-93+9\sqrt{113})/4$, one can conjecture (up to a plausible extension of [32]) the asymptotic estimate $U_n \sim c\Gamma^n n^{-\alpha}$, with $c > 0$ and $\alpha = 1 + \pi/\arccos(\xi) \approx 4.742$. By a criterion in [17] (ensuring that $\alpha \notin \mathbb{Q}$), this would imply that the generating function of U_n is not D-finite.

We now discuss the specialization to anti-diagonal rectangulations and Baxter permutations. We refer here to an *anti-diagonal rectangulation* as a rectangulation avoiding the patterns $\begin{smallmatrix} \bullet & \bullet \\ \bullet & \end{smallmatrix}$ and $\begin{smallmatrix} \bullet & \bullet \\ & \bullet \end{smallmatrix}$. Each weak class of rectangulations has a unique such representative, we see them here as a subclass of strong rectangulations and do not insist on considering the specific anti-diagonal representation on the $n \times n$ grid. Any anti-diagonal rectangulation has fiber of size 1, so that the corresponding history quadrant excursion is leftright. We also recall from the remark at the end of Section 4.4 that the mapping γ_s specializes into a bijection between Baxter permutations and anti-diagonal rectangulations.

Proposition 25. *The history quadrant excursions of length $n-1$ that encode Baxter permutations and anti-diagonal rectangulations of size n are in bijection with the set NIT_n of non-intersecting triples of lattice walks (with steps up or right), starting respectively at $(-1, 1), (0, 0), (1, -1)$, and ending at $(n-k-1, k), (n-k, k-1), (n-k+1, k-2)$ for some $1 \le k \le n$.*

Proof. Let σ be a history quadrant excursion, with $\mathcal{R}$ the rectangulation built from σ. The following properties are easy to check:

- If σ is leftmost, then each occurrence of $\begin{smallmatrix} \bullet & \bullet \\ \bullet & \end{smallmatrix}$ in $\mathcal{R}$ corresponds to a transition from a black or red point $p = (x, y)$ to a red or white point $p' = (x', y')$ such that $x' = x - 1$ (this corresponds to an insertion in a mixed valley in Figure 22).
- Symmetrically, if σ is rightmost, then each occurrence of $\begin{smallmatrix} \bullet & \bullet \\ & \bullet \end{smallmatrix}$ in $\mathcal{R}$ corresponds to a transition from a black or green point $p = (x, y)$ to a green or white point $p' = (x', y')$ such that $y' = y - 1$.

Hence, if σ is leftright, each occurrence of $\begin{smallmatrix} \bullet & \bullet \\ \bullet & \end{smallmatrix}$ in $\mathcal{R}$ corresponds to an occurrence of a special step $(-1, 2)$ or $(-1, 1)$, while each occurrence of $\begin{smallmatrix} \bullet & \bullet \\ & \bullet \end{smallmatrix}$ in R corresponds to an occurrence of a special step $(2, -1)$ or $(1, -1)$, so that $\mathcal{R}$ is anti-diagonal if and only if σ has no special step.

Note that a leftright quadrant excursion σ with no special step identifies to a quadrant walk of same length and with no colors on points, starting and ending at the origin, whose step-set is $\{2 \times (0, 0), (0, 1), (0, -1), (1, 0), (-1, 0), (-1, 1), (1, -1)\}$, with two kinds of stay-steps to account for the color of the initial point of each stay-step in σ. There is a simple bijection [24, Prop.20] between such walks of length $n - 1$ and NIT_n. □

Thus, we recover — via rectangulations — the fact that the Françon-Viennot encoding specialized to Baxter permutations yields a bijection with non-intersecting triples of lattice walks [83]. By the Gessel-Viennot Lemma, these are counted by the Baxter numbers B_n (whose exponential growth rate is 8).

[3] With the strong poset characterization it is not difficult to show that it also counts weak rectangulations of size n where every 2-sided segment (segment with at least one neighbor on each side) is given weight 2.

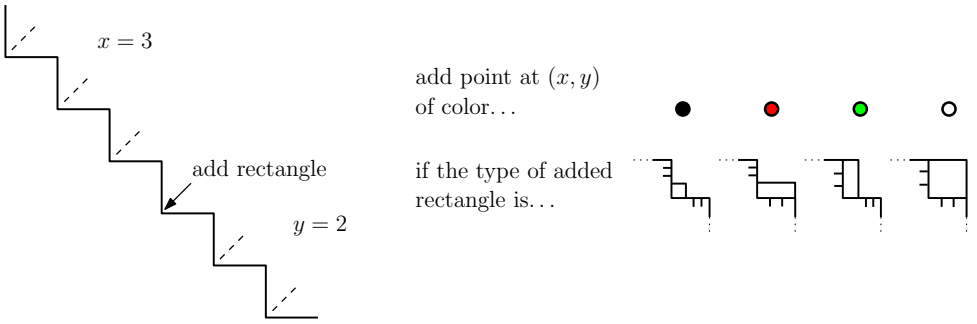

Figure 24: Correspondence between the insertion of a colored point in the quadrant and the insertion of a rectangle for weak rectangulations

To conclude the section, we briefly explain that a very similar study can be performed in the context of weak rectangulations. A weak rectangulation $\mathcal{R}$ endowed with a linear extension of its weak poset $P_w(\mathcal{R})$ can again be bijectively encoded by a history quadrant excursion, where the addition of a rectangle is now done in the "innermost" way in a valley for the situations without alignment of sides, see Figure 24 compared to Figure 20. Using the innermost convention yields the weak rectangulation in the form of its strong representative with no $\dashv$ nor $\perp$, the one for which the diagonal representation exists.

For the backward direction, in the current staircase shape, a rectangle is *available* if and only if all its adjacent rectangles are to its left or below. It is then easy to characterize the leftmost (resp. rightmost) history quadrant excursions in this context, i.e., those corresponding to weak rectangulations endowed with the leftmost (resp. rightmost) linear extension of their weak poset, equivalently at each step the last added rectangle is the rightmost (resp. leftmost) available one. Quite nicely, these have the same specification as the leftmost (resp. rightmost) walks in the strong case, upon replacing "and" by "or" in the first item. These quadrant walks of length $n-1$ also encode twisted (resp. co-twisted) Baxter permutations of size n. They are thus counted by B_n, even if a direct bijection to NIT_n does not seem easy to find.

As in the strong case, we can then consider the history quadrant walks that are leftmost and rightmost, called *leftright*. Leftright history quadrant excursions encode weak rectangulations whose weak poset is totally ordered. These are known to be the *one-sided* rectangulations, i.e., weak rectangulations such that for each segment at least one side has no contact, which are also the weak rectangulations with a unique strong representative. And they correspond via γ_w to the permutations in $\mathsf{Av}(\underline{2413}, \underline{2143}, \underline{3412}, \underline{3142})$, i.e., twisted and co-twisted Baxter permutations. By intersecting the step-sets for leftmost and rightmost walks, the specification of the step-set for leftright walks is as shown in Figure 25.

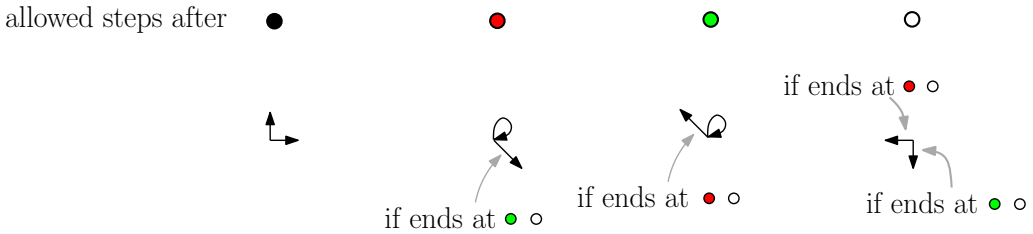

Figure 25: The allowed steps in leftright history quadrant walks, in the context of weak rectangulations.

Letting O_n be the number of one-sided rectangulations of size n, and number of leftright history quadrant excursions of length $n-1$, a recurrence for O_n analogue to the recurrence (3) for U_n can then be obtained, by first-step removal in closed leftright history quadrant walks. Another counting method for O_n, also in polynomial time, has been given in [20] (pages 162-175) by describing a generating tree for the permutation class, the sequence starts with $1, 2, 6, 20, 72, 274, 1088, 4470, 18884, 81652, \ldots$ and is OEIS A348351.

Proposition 26. *The exponential growth rate of O_n is bounded from above by $\Gamma' := \frac{1}{2}(7+\sqrt{17}) \approx 5.562$.*

Proof. Let

$$\mathbb{A}' = \begin{pmatrix} 2 & 2 & 2 & 2 \\ 1 & 1 & 2 & 2 \\ 1 & 2 & 1 & 2 \\ 0 & 1 & 1 & 2 \end{pmatrix}$$

and let $\mathbb{I} = (1,1,1,1)$. The number of leftright walks of length n (starting at the origin) with no constraint on domain nor on endpoint is equal to $\mathbb{I} \cdot \mathbb{A}'^{\,n} \cdot \mathbb{I}^T$; and Γ' is the spectral radius of $\mathbb{A}'$. □

Again, by similar calculations as [48, Conjecture 25], letting $\xi' = (-29+7\sqrt{17})/4$, one can conjecture the asymptotic estimate $O_n \sim c'\,\Gamma'^{\,n} n^{-\alpha'}$, with $c' > 0$ and $\alpha' = 1 + \pi/\arccos(\xi') \approx 2.957$, which would imply that the generating function of O_n is not D-finite.

An interesting consequence of Proposition 26 is that the growth rate of one-sided rectangulations, which are also the rectangulations that are *area-universal* [38], is smaller than the known [80, 47] growth rate $27/4 = 6.75$ of triangulations of the 4-gon that are irreducible (no separating triangle). Thus the irreducible triangulations of the 4-gon admitting a dual representation as an area-universal rectangulation are exponentially rare, their growth rate being at most Γ'.

5 Guillotine rectangulations

In this section we deal with guillotine rectangulations, introduced in Section 2.5. While weak guillotine rectangulations are well understood (see Propositions 3 and 4), we are not aware of any results concerning strong guillotine rectangulations. In this section we provide a uniform treatment of guillotine rectangulations by characterizing those permutations that correspond to guillotine partitions under both permutation-to-rectangulation mappings γ_w and γ_s, by means of pattern avoidance. As a result, we can restrict all the bijections between (both weak and strong) rectangulations that were mentioned above, to the guillotine case. In particular, we find a permutation class bijective to *strong guillotine rectangulations*.

5.1 Characterization by mesh patterns

Consider the following mesh patterns[4] (depicted in Figure 26):

$$p_1 = (25314,\ \{(0,3),(0,4),(1,3),(4,2),(5,1),(5,2)\}),$$
$$p_2 = (41352,\ \{(0,1),(0,2),(1,2),(4,3),(5,3),(5,4)\}).$$

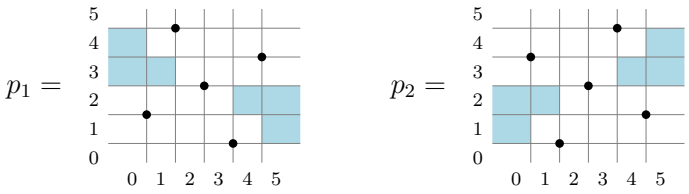

Figure 26: Two mesh patterns whose avoidance characterizes guillotine permutations.

Theorem 27. *Let $\pi \in S_n$. Then the following conditions are equivalent:*

(1) The weak rectangulation $\gamma_w(\pi)$ is guillotine,

(2) The strong rectangulation $\gamma_s(\pi)$ is guillotine,

(3) π avoids both mesh patterns p_1 and p_2.

[4] These mesh patterns were proposed by Merino and Mütze [58], see remark after Corollary 32.

The equivalence of (1) and (2) is clear, since being guillotine is invariant under shuffling. Hence, it suffices to prove the equivalence of (1) and (3). Recall from Proposition 3 that a rectangulations is guillotine if and only if it avoids two "windmills" $\boxplus$ and $\boxplus$. Theorem 27 follows directly from the following lemma, which also precisely points out the correspondence between both mesh patterns and both kinds of windmills.

Lemma 28. *Let $\pi \in S_n$.*

(a) $\gamma_w(\pi)$ contains $\boxplus$ if and only if π contains p_1,

(b) $\gamma_w(\pi)$ contains $\boxplus$ if and only if π contains p_2.

Proof. We provide the proof for (a) (then (b) follows from (a) by reflection via Observation 19).

At the first step we modify the pattern p_1 in a way that simplifies some technical details. Consider the mesh pattern

$$q_1 = (25314,\ \{0,1\} \times \{2,3,4\}\ \cup\ \{4,5\} \times \{1,2,3\}).$$

We show that a permutation π contains p_1 if and only if it contains q_1, refer to Figure 27. Assume that π contains p_1, and the pattern 25314 of p_1 is realized as $becad$ where $a < b < c < d < e$. Then, in the plot, we can replace the point e by a left-minimum point in the cell $(1,4)$, then b by the top-most point in $(0,2) \cup (1,2)$, then a by a right-maximum point in $(4,1)$, and finally d by the bottom-most point in $(4,3) \cup (5,3)$. This shows that if a permutation contains p_1 then it contains q_1. The converse implication is trivial.

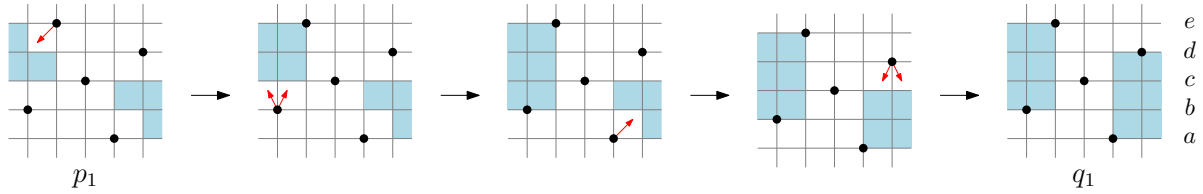

Figure 27: An occurrence of p_1 implies an occurrence of q_1.

We now prove that $\gamma_w(\pi)$ contains $\boxplus$ if and only if π contains q_1.

($\Leftarrow$) Let π be a permutation that contains q_1, and consider the diagonal representative of $\gamma_w(\pi)$. Assume, as above, that the pattern 25314 of p_1 is realized as $becad$. The shaded regions of q_1 imply that no rectangle r_x with label x such that $b < x < e$ is inserted earlier than e, and that no rectangle r_x with $a < x < d$ is inserted later than a. It follows that just after inserting the rectangle r_e, the staircase contains a horizontal segment s_e just above r_e and a vertical segment s_b just to the right from r_b, and these segments (shown by red in Figure 28) meet in a $\vdash$ joint. Similarly, just before inserting the rectangle r_a, the staircase contains a horizontal segment s_a just under r_a and a vertical segment s_d just to the left from r_d, and these segments (shown by green in Figure 28) meet in a $\dashv$ joint. Due to the presence of r_c, we know that s_d does not coincide with s_b.

Now we show that $\gamma_w(\pi)$ contains a windmill $\boxplus$. Traverse the segment s_b from below to above. Due to s_a, the segment s_b can not reach the upper side of R, as it is blocked by a horizontal segment $s_{a'}$ (which is possibly s_a). Now we traverse $s_{a'}$ to the right. Due to the existence of s_d, the segment $s_{a'}$ cannot reach the right side of R, as it is be blocked by a vertical segment $s_{d'}$ (which is possibly s_d). We continue traversing segments in this way and due to s_a, s_d, s_e, s_b we never reach the boundary of R. Since the process is finite, a windmill $\boxplus$ will eventually be obtained.

($\Rightarrow$) Let $\mathcal{R}$ be a rectangulation containing $\boxplus$. Label by r_a, r_b, r_d, r_e the rectangles as shown in Figure 29: r_a is the rectangle whose bottom-right corner is the top-right corner of the windmill, r_d is the upmost rectangle whose left side is included in the right vertical segment of the windmill, and similarly for r_e and r_b. Finally, let r_c be any rectangle in the region bounded by the windmill. Then we have $a < b < c < d < e$ in the diagonal ordering. On the other hand, in $P_w(\mathcal{R})$ we have $b \prec_w e \prec_w c \prec_w a \prec_w d$, which gives the pattern 25314 in any linear extension π of this poset. It remains to show that there are no points in the shaded regions from the plot of q_1. Suppose there is a point in the region $\{0,1\} \times \{2,3,4\}$.

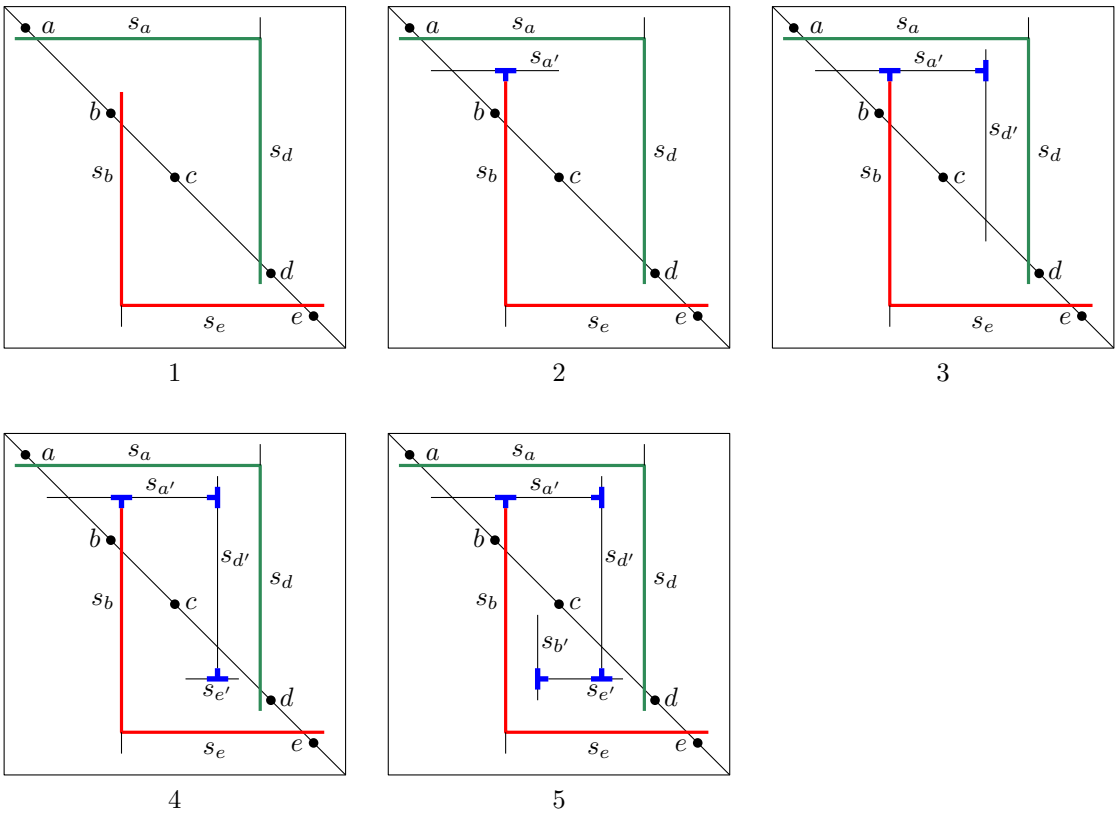

Figure 28: Illustration for ($\Leftarrow$) in the proof of Theorem 27: q_1 implies $\pitchfork$.

Then there exists a rectangle r_x such that $b < x < e$, which is inserted earlier than e. By Observation 1(1), all rectangles r_x such that $b < x < e$ are contained in the region shown in grey in Figure 29. However, all rectangles r_x included in this region satisfy $e \prec_w x$, hence r_x can not be inserted earlier than r_e. □

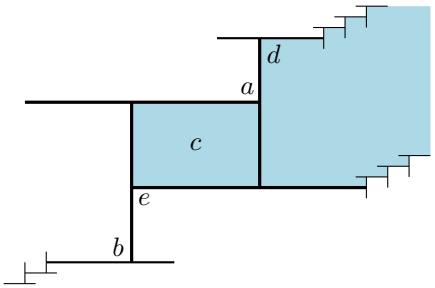

Figure 29: Illustration for ($\Rightarrow$) in the proof of Theorem 27: $\pitchfork$ implies q_1.

5.2 New bijections and permutation classes for guillotine rectangulations

In this section we discuss specializations of the bijections β_{TB}, β_{CTB}, β_{B}, β_{2C}, β_{C2C} from Theorems 7 and 15 to the case of guillotine rectangulations.

Weak guillotine rectangulations. Basically, the respective permutation classes are obtained by adding p_1 and p_2 to the forbidden patterns. The next lemma makes it possible to describe some of them by fewer patterns.

Lemma 29. *The following identities between permutation classes hold:*

1. $\mathsf{Av}(\underline{24}13, \underline{34}12, p_1) = \mathsf{Av}(2413, \underline{34}12)$,
2. $\mathsf{Av}(\underline{24}13, \underline{31}42, p_1) = \mathsf{Av}(2413, \underline{31}42)$,
3. $\mathsf{Av}(\underline{31}42, \underline{21}43, p_2) = \mathsf{Av}(3142, \underline{21}43)$,
4. $\mathsf{Av}(\underline{31}42, \underline{24}13, p_2) = \mathsf{Av}(3142, \underline{24}13)$.

Proof. We provide a detailed proof of (1). The proof of (2) is similar, and the proofs of (3) and (4) are obtained by taking complements.

In (1), the implication $\supseteq$ is obvious. To prove $\subseteq$, we need to show that if π contains 2413, then it contains $\underline{24}13$, $\underline{34}12$, or p_1.

Let $bead$, where $a < b < d < e$, be a *(vertically) shortest* occurrence of 2413, that is, an occurrence with the smallest possible $e - a$. If it is not a part of 25314, then we can replace the point e by the rightmost point in the region $(2,3) \cup (2,4)$; this yields an occurrence of $\underline{24}13$ (refer to the left part of Figure 30).

Now assume that our occurrence of 2413 is a part of 25314 (refer to the right part of Figure 30). The regions $(1,4)$, $(2,4)$, $(3,4)$, $(0,3)$, $(1,3)$, $(4,2)$, $(5,2)$, $(2,1)$, $(3,1)$, $(4,1)$ are empty because otherwise we have a shorter occurrence of the pattern 2413. If the region $(0,4)$ is not empty, then — applying the same argument as above and using the fact that the region $(2,4)$ is empty — we obtain an occurrence of $\underline{34}12$. Similarly, we obtain $\underline{34}12$ if $(5,1)$ is not empty. And if both regions $(0,4)$ and $(5,1)$ are empty, then our assumed 25314 is an occurrence of p_1. □

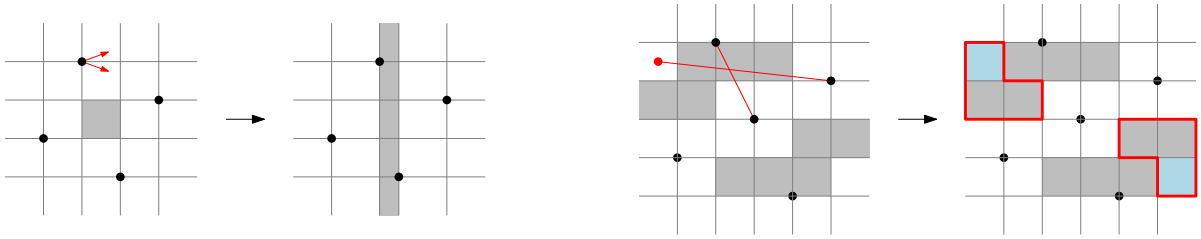

Figure 30: Illustration to the proof of Lemma 29.

Remark. Note that it is not possible to "cancel" the patterns that occur on both sides of these identities. For example, $\mathsf{Av}(\underline{24}13, p_1) = \mathsf{Av}(2413)$ is false: 526314 is a counterexample.

Combining Lemma 29 with Lemma 28 we obtain:

Proposition 30. *The following families of permutations are in bijection (respectively via β_{TB}, β_{CTB}, and β_{B}) with weak rectangulations that avoid $\boxplus$:*

1. $\mathsf{Av}(2413, \underline{34}12)$,
2. $\mathsf{Av}(\underline{21}43, \underline{31}42, p_1)$,
3. $\mathsf{Av}(2413, \underline{31}42)$.

Similarly, via β_{TB}, β_{CTB}, and β_{B}, weak rectangulations that avoid $\boxplus$ correspond respectively to the families $\mathsf{Av}(\underline{24}13, \underline{34}12, p_2)$, $\mathsf{Av}(\underline{21}43, 3142)$, and $\mathsf{Av}(\underline{24}13, 3142)$.

Proposition 30 sheds new light on some previously known results. Weak rectangulations of size n are in a simple bijection with 2-orientations [31] on rooted simple quadrangulations (embedded on the sphere) with $n+1$ faces, i.e., orientations of the edges not incident to the root-face such that vertices not incident (resp. incident) to the root-face have outdegree 2 (resp. 0). Moreover, a weak rectangulation has a $\boxplus$ if and only if the 2-orientation has a clockwise cycle (more precisely, the occurrence of a $\boxplus$ corresponds to the occurrence of a clockwise 4-cycle, and the presence of a clockwise cycle implies the presence of a clockwise 4-cycle). Since any rooted simple quadrangulation has a unique 2-orientation with no clockwise cycle [64, 40], weak rectangulations of size n with no $\boxplus$ are thus in bijection with rooted simple quadrangulations with $n+1$ faces, which are themselves in bijection with rooted non-separable maps with $n+1$ edges, whose counting coefficients are $a_n = \frac{2\,(3n)!}{(n+1)!\,(2n+1)!}$ as shown in [81, 68].

The fact that $\mathsf{Av}(2413, 3\underline{14}2)$ is in bijection with rooted non-separable maps was already proved in [36] (via isomorphic generating trees) and in [15], by specializing a bijection between Baxter permutations and plane bipolar orientations: this bijection has the property that Baxter permutations with no 2413 correspond to plane bipolar orientations with no ROP (right-oriented piece), and moreover any rooted non-separable map has a unique plane bipolar orientation with no ROP. Our bijection between $\mathsf{Av}(2413, 3\underline{14}2)$ and weak rectangulations with no $\pitchfork$ is very analogous, since plane bipolar orientations are in a simple bijection [31] with 2-orientations, such that the occurrence of a ROP corresponds to the occurrence of a counterclockwise 4-cycle (or the occurrence of a clockwise 4-cycle, upon reflection).

Let us also mention that the coefficients a_n are well-known to count 2-stack sortable permutations [86]. In [35], a correspondence with $\mathsf{Av}(2413, 3\underline{14}2)$ has been obtained via a chain of several bijections relating permutation classes (and relying on isomorphic generating trees). Along that chain after $\mathsf{Av}(2413, 3\underline{14}2)$ is the class $\mathsf{Av}(2413, 3\underline{41}2)$ (see [35, Fig.3]); this corresponds to the link between the first and second item in Proposition 30. Recently a more direct bijective link between 2-stack sortable permutations and rooted non-separable maps has been established via *fighting fish* [39, 34].

We now further specialize the bijections (for weak classes) to the guillotine case:

Proposition 31. *The following families of permutations are in bijection (respectively via β_{TB}, β_{CTB}, and β_{B}) with weak guillotine rectangulations:*

1. $\mathsf{Av}(2413, 3\underline{41}2, p_2)$,
2. $\mathsf{Av}(2\underline{14}3, 3142, p_1)$,
3. $\mathsf{Av}(2413, 3142)$.

Proof. It follows from Theorems 7 and 27 that weak guillotine rectangulations are in bijection (respectively via β_{TB}, β_{CTB}, and β_{B}) with $\mathsf{Av}(2\underline{41}3, 3\underline{41}2, p_1, p_2)$, $\mathsf{Av}(2\underline{14}3, 3\underline{14}2, p_1, p_2)$, and $\mathsf{Av}(2\underline{41}3, 3\underline{14}2, p_1, p_2)$. By Lemma 29 we have

$$\mathsf{Av}(2\underline{41}3, 3\underline{41}2, p_1, p_2) = \mathsf{Av}(2413, 3\underline{41}2, p_2), \qquad \mathsf{Av}(2\underline{41}3, 3\underline{41}2, p_1, p_2) = \mathsf{Av}(2413, 3\underline{41}2, p_2),$$
$$\mathsf{Av}(2\underline{41}3, 3\underline{14}2, p_1, p_2) = \mathsf{Av}(2\underline{41}3, 3142, p_1), \qquad \mathsf{Av}(2\underline{14}3, 3\underline{14}2, p_1, p_2) = \mathsf{Av}(2\underline{14}3, 3142, p_1).$$

The combination of the two identities for $\mathsf{Av}(2\underline{41}3, 3\underline{14}2, p_1, p_2)$ implies that this class is equal to $\mathsf{Av}(2413, 3142)$. □

Part 3 of Proposition 31 recovers the bijection β_{S} from Theorem 7(4); parts 1 and 2 are new results.

Strong guillotine rectangulations. Here we just add p_1 and p_2 to the patterns that define 2-clumped permutations and co-2-clumped permutations, and we did not find a way to describe these classes with fewer patterns. However, **this is the first known representation of strong guillotine rectangulations by permutation classes**.

Proposition 32. *The following families of permutations are in bijection (respectively via β_{2C} and β_{C2C}) with strong guillotine rectangulations:*

1. *the $\{p_1, p_2\}$-avoiding 2-clumped permutations,*
2. *the $\{p_1, p_2\}$-avoiding co-2-clumped permutations.*

Summary. Proposition 32(1) was conjectured and communicated to us by Merino and Mütze [58]. They found the mesh patterns p_1 and p_2 experimentally, as a part of their study of patterns in rectangulations. This conjecture was our starting point for the study presented in this section. As our results — mainly Theorem 27 and Lemma 28 — show, these two patterns not just define a permutation class in bijection with with strong guillotine rectangulations, but they generally "encode the windmills in the language of permutations". As such, these results belong to the study of representing patterns in rectangulations by patterns in permutations, which was suggested in [59, Section 11] as an open question. Our Lemma 16 is another instance of correspondence between these kinds of patterns, see also [5] for more results of this kind.

5.3 Enumeration of strong guillotine rectangulations

Generating the enumerating sequence. A straightforward way to generate the enumerating sequence for strong guillotine rectangulations is counting multiplicities. A *multiplicity* of a weak rectangulation $\mathcal{R}$ is the number of strong rectangulations whose union constitutes $\mathcal{R}$. Every segment s contributes $\binom{a+b}{a}$ to the multiplicity of $\mathcal{R}$, where a and b are the numbers of neighbors of s from both sides. The total multiplicity of a rectangulation $\mathcal{R}$ is the product of such binomial coefficients taken over all its segments.

For strong guillotine rectangulations, we can use the same argument as in our proof of Proposition 4, but taking into account the multiplicities. Let $\mathcal{R}$ be a vertical guillotine rectangulation of size > 1, and let s be its leftmost cut. Denote by $\mathcal{R}_L$ and $\mathcal{R}_R$ the left and the right subrectangulations separated by s. If the multiplicity of $\mathcal{R}_L$ is m_1, and that of $\mathcal{R}_R$ is m_2, then the multiplicity of $\mathcal{R}$ is $m_1 m_2 \binom{a+b}{a}$, where a and b are the numbers of left and right neighbors of s.

Therefore, we have to keep track of the numbers of segments that have an endpoint on the sides of R. This leads to a recurrence in five variables. Denote by $S(n,\ell,t,r,b)$ the number of strong guillotine rectangulations of size n with ℓ, t, r, b endpoints of segments on the left, top, right, bottom side. Further, denote by $S_V(n,\ell,t,r,b)$ and $S_H(n,\ell,t,r,b)$ the numbers of vertical and, respectively, horizontal strong guillotine rectangulations with these parameters. (To keep the expressions more compact, here we regard the rectangulation of size 1 as both vertical and horizontal.) Then we have the following recurrence.

For $n = 1$:

$$S(1,\ell,t,r,b) = S_V(1,0,0,0,0) = S_H(1,0,0,0,0) = \begin{cases} 1, & (\ell,t,r,b) = (0,0,0,0), \\ 0, & (\ell,t,r,b) \neq (0,0,0,0). \end{cases}$$

For $n > 1$:

$$S_V(n,\ell,t,r,b) = \sum S_H(n',\ell,t',r',b') \cdot S(n-n',\ell',t-1-t',r,b-1-b') \cdot \binom{r'+\ell'}{r'},$$

where the sum is taken over $1 \le n' \le n-1$ and $0 \le t', r', b', \ell' \le n$.

This rule is illustrated in Figure 31.

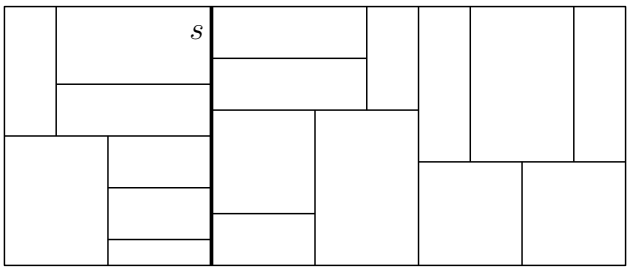

Figure 31: Illustration of the recurrence for counting strong guillotine rectangulations. The multiplicity of this rectangulation is the product of the multiplicity of the left part, the multiplicity of the right part, and the binomial coefficient $\binom{7}{4}$.

For $S_H(n,\ell,t,r,b)$ we have a similar expression, but for computations we can use

$$S_V(n,\ell,t,r,b) = S_V(n,r,t,\ell,b) = S_V(n,\ell,b,r,t) = S_V(n,r,b,\ell,t) =$$
$$= S_H(n,t,\ell,b,r) = S_H(n,b,\ell,t,r) = S_H(n,t,r,b,\ell) = S_H(n,b,r,t,\ell).$$

Finally, for $n > 1$ we have

$$S(n,\ell,t,r,b) = S_H(n,\ell,t,r,b) + S_V(n,\ell,t,r,b)$$

We implemented the recurrence in Maple, and obtained the first numbers in the enumerating sequence of strong guillotine rectangulations of size n:

$n=1\dots8$	$n=9\dots16$	$n=17\dots24$	$n=25\dots32$
1	138100	1143606856808	23673987861077379184
2	926008	9072734766636	201493429381831155064
6	6418576	72827462660824	1725380127954612191928
24	45755516	590852491725920	14858311852609658166276
114	334117246	4840436813758832	12863472331844387526170 6
606	2491317430	40009072880216344	11192036625813491298002 54
3494	18919957430	333419662183186932	97834773148006549419371 82
21434	146034939362	2799687668599080296	85899976772035554402923170

This sequence has no OEIS entry at the time of writing.

Asymptotic bounds. We now would like to show that guillotine rectangulations are rare among strong rectangulations of size n, as n gets large. Precisely, we will show that the exponential growth rate of strong guillotine rectangulations is bounded from above by a constant ≈ 13.081, hence is strictly smaller than the exponential growth rate of all strong rectangulations, which, as mentioned above, is known to be $27/2$ [49].

We will make use of asymptotic results in [49] (to be slightly extended below in Lemma 33) on so-called *arbitrary rectangulations*, which are rectangulations allowing for points where 4 rectangles meet, called *special points*. These are considered in the strong equivalence sense. Let $a_{n,k}$ be the number of arbitrary rectangulations of size n with k special points, let $a_n(v) = \sum_k a_{n,k} v^k$, and let $A(z,v) = \sum_n a_n(v) z^n$ be the associated counting series. For fixed v, let $\rho(v)$ be the radius of convergence of $z \to A(z,v)$, i.e., $1/\rho(v)$ is the exponential growth rate of $a_n(v)$. It has been shown in [49, Thm. 4.3] that, for $v \geq 0$,

$$\rho(v) = \frac{2(2+v)}{2v^2+18v+27+(9+4v)^{3/2}}. \tag{4}$$

Lemma 33. *There exist non-negative coefficients $\tilde{a}_{n,k}$ such that, with $\tilde{a}_n(v) := \sum_k \tilde{a}_{n,k} v^k$, we have $a_n(v) = \tilde{a}_n(v+2)$, so that $a_n(v) \geq 0$ for $v \geq -2$. Moreover, for $v \in (-2,0)$, $\rho(v)$ is still given by* (4).

Proof. An arbitrary rectangulation is called *reduced* if it avoids both $\dashv\!\vdash$ and $\vdash\!\dashv$. If we let $\tilde{a}_{n,k}$ be the number of reduced arbitrary rectangulations of size n with k special points, and let $\tilde{a}_n(v) = \sum_k \tilde{a}_{n,k} v^k$, then we have

$$a_n(v) = \tilde{a}_n(v+2).$$

Indeed, an arbitrary rectangulation yields a reduced one by contracting the inner segment of each $\dashv\!\vdash$ or $\vdash\!\dashv$, turning it into a $+$. Conversely, a reduced arbitrary rectangulation lifts to a set of arbitrary rectangulations by choosing, for each special point $+$, whether it stays unchanged, is expanded into $\dashv\!\vdash$, or is expanded into $\vdash\!\dashv$.

The encoding of arbitrary rectangulations by weighted quadrant walks that is obtained in [49, Sec.2.4] (relying on a bijection in [52]) can be specialized to reduced arbitrary rectangulations: with the terminology of [49] (where the study is done in the dual setting of transversal structures), forbidding $\vdash\!\dashv$ amounts to forbidding consecutive face-steps, and forbidding $\dashv\!\vdash$ can easily be encoded in the weight affected to face-steps. All calculations done as in [49, Sec.4] (details omitted) one finds that, if $\tilde{\rho}(v)$ denotes the radius of convergence of $v \to \sum_n \tilde{a}_n(v) z^n$ for $v > 0$ (which equals $\rho(v-2)$ since $\tilde{a}_n(v) = a_n(v-2)$), then the obtained expression of $\tilde{\rho}(v)$ matches the right-hand side of (4) where v is substituted by $v-2$. □

In a strong rectangulation the *enclosing 4-gon* of a windmill is the 4-gon extracted from the union of the 4 constituting segments. The windmill is called *simple* if there is no segment leaving a point on a side of the enclosing 4-gon towards the exterior of the 4-gon. A *small windmill* is a simple windmill with a single rectangular region inside the enclosing 4-gon. Let b_n be the number of rectangulations of size n with no small windmill. Obviously, b_n is an upper bound on the number of guillotine rectangulations of size n.

Proposition 34. *The exponential growth rate of b_n is bounded from above by the unique positive root $x_0 \approx 13.155$ of the polynomial $2x^5 - 29x^4 + 36x^3 - 8x^2 - 8$.*

Proof. Let $\hat{a}_{n,k}$ be the number of rectangulations of size n with k small windmills; and let $\hat{A}(z,v) = \sum_{n,k} \hat{a}_{n,k} z^n v^k$ be the associated counting series. Then we have $A(z,2vz) = \hat{A}(z,1+v)$. Indeed, starting from an arbitrary rectangulation, each special point $+$ can be expanded into either $\dashv\vdash$ or $\vdash\dashv$ (here these symbols are to be understood as small windmills); then these form an arbitrary subset of all small windmills in the obtained rectangulation. Hence, letting $B(z) = \sum_n b_n z^n$, we have

$$B(z) = \hat{A}(z,0) = A(z,-2z).$$

For $0 \le z \le 1$ such that $z < \rho(-2z)$, the function $A(.,.)$ is analytic at $(z,-2z)$ (this follows from the fact that, by continuity of $\rho(.)$, there exist $\epsilon, \eta > 0$ such that $\sum_{n,k} \tilde{a}_{n,k}(z+\epsilon)^n(2-2z+\eta)^k < +\infty$). Hence $B(.)$ is analytic at z. Thus, letting z_0 be the smallest positive root of the equation $z = \rho(-2z)$, the function $B(.)$ is analytic at z for $0 \le z < z_0$. By Pringsheim's theorem, the radius of convergence of $B(z)$ is at least z_0, hence the exponential growth rate of b_n is at most $1/z_0$. From the above expression of $\rho(v)$, we find that $1/z_0 \approx 13.155$ is the unique positive root of the polynomial $2x^5 - 29x^4 + 36x^3 - 8x^2 - 8$. □

Now let $\bar{b}_n$ be the number of rectangulations of size n with no simple windmill, which again is an upper bound on the number of guillotine rectangulations of size n.

Proposition 35. *The exponential growth rate of $\bar{b}_n$ is bounded from above by* 13.081.

Proof. For any fixed $k \ge 1$, a simple windmill is called *k-small* if the rectangulation inside the enclosing 4-gon is a guillotine rectangulation of size at most k. Let $b_n^{(k)}$ be the number of rectangulations of size n with no k-small windmill (in particular $b_n = b_n^{(1)}$, and $\bar{b}_n \le b_n(k)$ for all $k \ge 1$); let $B^{(k)}(z) = \sum_n b_n^{(k)} z^n$. With $g_n := S(n)$ the number of guillotine rectangulations of size n, the argument in Proposition 34 extends to give the equation

$$B^{(k)}(z) = A\Big(z, -2\sum_{i=1}^{k} g_i z^i\Big).$$

Letting $z_0^{(k)}$ be the smallest positive solution of the equation $z = \rho(-2\sum_{i=1}^k g_i z^i)$, by the same argument as in Proposition 34, the radius of convergence of $B^{(k)}(z)$ is at least $z_0^{(k)}$, hence $1/z_0^{(k)}$ is an upper bound on the exponential growth rate of $b_n^{(k)}$, and also of $\bar{b}_n \le b_n^{(k)}$. We find that as k increases, $1/z_0^{(k)}$ (which decreases) rapidly approaches a constant ≈ 13.081 (upper approximation). □

Remark. For fixed n, $b_n^{(k)}$ weakly decreases with k and stabilizes to $\bar{b}_n$. We expect that (for any fixed $k \ge 1$) $1/z_0^{(k)}$ is the exponential growth rate of $b_n^{(k)}$, and that, as $k \to \infty$, it converges to the exponential growth rate of $\bar{b}_n$, which thus should be ≈ 13.081. However, forbidding only simple windmills does not seem to give a close upper bound on the exponential growth rate of guillotine rectangulations. Indeed, from the table of the initial counting coefficients g_n, and applying acceleration of convergence (see, e.g., [50, Sec.6]) to the ratio g_{n+1}/g_n, the exponential growth rate of g_n seems to be ≈ 10.24.

Finally, we discuss lower bounds. By Proposition 4, the number of weak guillotine rectangulations of size n is the $(n-1)$th Schröder number. Therefore, the exponential growth rate of Schröder numbers, $3 + 2\sqrt{2} \approx 5.828$, is a "trivial" lower bound on the exponential growth rate of strong guillotine rectangulations. In order to give a better bound, we consider weak guillotine rectangulations where every 2-sided segment (that is, a segment with at least one neighbor on each side) has weight 2. This will give a lower bound, since the neighbors of every 2-sided segment can be shuffled in at least two ways. We adapt the decomposition from our proof of Proposition 4 as follows. Let $G = G(x,y)$ be the generating function for weak guillotine rectangulations, where the variable x is for the size, and y for the number of 2-sided segments. Further, let $G_0 = G_0(x,y)$ be the generating function for weak guillotine rectangulations that have *no segment* with an endpoint on the left side of R, and let $G_1 = G_1(x,y)$ be the generating function for weak guillotine rectangulations that have *at least one segment* with an endpoint on the left side of R. Finally, let $H = H(x,y)$ and $V = V(x,y)$ be the generating functions for horizontal and, respectively, vertical weak guillotine rectangulations. Then we have $H = V$, $G = x + H + V$, $G_0 = xG + x$, and $G_1 = (1-x)G - x$, and the decomposition of a vertical guillotine rectangulation by its leftmost cut leads to the following weighted version of equation (1):

$$V = xG + H\Big(G_0 + yG_1\Big).$$

The solution of this system yields

$$G(x,2) = \frac{1+x-x^2-\sqrt{1-6x-5x^2+2x^3+x^4}}{2(2-x)},$$

and its dominant singularity gives us the following lower bound.

Proposition 36. *The exponential growth rate of the number of strong guillotine rectangulations is bounded from below by* $\frac{1}{2}\left(1+\sqrt{13-8\sqrt{2}}\right)\left(3+2\sqrt{2}\right) \approx 6.699$.

This strategy can be pushed further: for a fixed threshold value $t \geq 1$, every segment with i neighbors on one side and j neighbors on the other side is weighted by $\binom{i'+j'}{i'}$, where $i' = \min(i,t)$ and $j' = \min(j,t)$. The exponential growth rate for any fixed t should be computable (by the approach of [43, VII.6.3]), and grow with t, giving better and better lower bounds. The complexity of the decomposition and of computations, however, will rapidly explode as t grows.

Acknowledgments

The work on this paper began during the *Order & Geometry Workshop*, Ciążeń, Poland, 13–18 September 2022. The research of Andrei Asinowski is partially supported by FWF — The Austrian Science Fund, grant P32731. The research of Stefan Felsner is partially supported by grant DFG FE 340/13-1. The research of Éric Fusy is partially supported by the projects ANR-20-CE48-0018 (3DMaps) and ANR-19-CE48-0011 (COMBINÉ).

References

[1] Michio Abe. Covering the square by squares without overlapping. *J. Japan Math. Phys.*, 4:359–366, 1930.

[2] Michio Abe. On the problem to cover simply and without gap the inside of a square with a finite number of squares which are all different from one another. *Proc. Phys.-Math. Soc. Japan*, 14:385–387, 1932.

[3] Eyal Ackerman, Gill Barequet, and Ron Y. Pinter. A bijection between permutations and floorplans, and its applications. *Discret. Appl. Math.*, 154(12):1674–1684, 2006.

[4] Eyal Ackerman, Gill Barequet, Ron Y. Pinter, and Dan Romik. The number of guillotine partitions in d dimensions. *Inf. Process. Lett.*, 98(4):162–167, 2006.

[5] Andrei Asinowski and Cyril Banderier. From geometry to generating functions: rectangulations and permutations. arXiv:2401.05558.

[6] Andrei Asinowski, Gill Barequet, Mireille Bousquet-Mélou, Toufik Mansour, and Ron Y. Pinter. Orders induced by segments in floorplans and (2–14–3, 3–41–2)-avoiding permutations. *Electron. J. Comb.*, 20(2):35, 2013.

[7] Andrei Asinowski and Toufik Mansour. Separable d-permutations and guillotine partitions. *Annals of Combinatorics*, 14:17–43, 2010.

[8] Kirby A. Baker, Peter C. Fishburn, and Fred S. Roberts. Partial orders of dimension 2. *Networks*, 2(1):11–28, 1972.

[9] Glen Baxter. On fixed points of the composite of commuting functions. *Proc. AMS*, 15(6):851–855, 1964.

[10] Glen Baxter and James T. Joichi. On permutations induced by commuting functions, and an embedding question. *Math. Scandin.*, 13:140–150, 1963.

[11] Olivier Beaumont, Vincent Boudet, Fabrice Rastello, and Yves Robert. Partitioning a square into rectangles: NP-completeness and approximation algorithms. *Algorithmica*, 34(3):217–239, 2002.

[12] Benjamin B. Bederson, Ben Shneiderman, and Martin Wattenberg. Ordered and quantum treemaps: Making effective use of 2D space to display hierarchies. *ACM Trans. Graph.*, 21(4):833–854, 2002.

[13] David Bevan. Permutation patterns: basic definitions and notation, 2015. arXiv:1506.06673.

[14] Anders Björner and Michelle L. Wachs. Permutation statistics and linear extensions of posets. *J. Comb. Theory, Ser. A*, 58(1):85–114, 1991.

[15] Nicolas Bonichon, Mireille Bousquet-Mélou, and Éric Fusy. Baxter permutations and plane bipolar orientations. *Séminaire Lotharingien de Combinatoire*, 61:B61Ah, 2010.

[16] Prosenjit Bose, Jonathan F. Buss, and Anna Lubiw. Pattern matching for permutations. *Inf. Process. Lett.*, 65(5):277–283, 1998.

[17] Alin Bostan, Kilian Raschel, and Bruno Salvy. Non-D-finite excursions in the quarter plane. *J. Comb. Theory, Ser. A*, 121:45–63, 2014.

[18] Mireille Bousquet-Mélou. Four classes of pattern-avoiding permutations under one roof: Generating trees with two labels. *The Electron. J. Comb.*, 9(2):R19, 2003.

[19] Mathilde Bouvel, Veronica Guerrini, Andrew Rechnitzer, and Simone Rinaldi. Semi-Baxter and Strong-Baxter: Two Relatives of the Baxter Sequence. *SIAM J. Discret. Math.*, 32(4):2795–2819, 2018.

[20] Mathilde Bouvel, Veronica Guerrini, and Simone Rinaldi. Avoiding Baxter-like patterns. *The 17th Conference on Permutation Patterns*, June 2019, Zürich, Switzerland.

[21] Petter Brändén and Anders Claesson. Mesh patterns and the expansion of permutation statistics as sums of permutation patterns. *Electron. J. Comb.*, 18(2), 2011.

[22] R. Leonard Brooks, Cedric A. B. Smith, Arthur H. Stone, and William T. Tutte. The dissection of rectangles into squares. *Duke Math. J.*, 7:312–340, 1940.

[23] Kevin Buchin, Bettina Speckmann, and Sander Verdonschot. Evolution strategies for optimizing rectangular cartograms. In Ningchuan Xiao, Mei-Po Kwan, Michael F. Goodchild, and Shashi Shekhar, editors, *Proc. GIScience 2012*, volume 7478 of *LNCS*, pages 29–42. Springer, 2012.

[24] Sophie Burrill, Julien Courtiel, Éric Fusy, Stephen Melczer, and Marni Mishna. Tableau sequences, open diagrams, and Baxter families. *Europ. J. Comb.*, 58:144–165, 2016.

[25] Felipe C. Calheiros, Abilio Lucena, and Cid C. de Souza. Optimal rectangular partitions. *Networks*, 41(1):51–67, 2003.

[26] Jean Cardinal, Vera Sacristán, and Rodrigo I. Silveira. A note on flips in diagonal rectangulations. *Discret. Math. Theor. Comput. Sci.*, 20(2), 2018.

[27] Cesar Ceballos, Francisco Santos, and Günter M. Ziegler. Many non-equivalent realizations of the associahedron. *Comb.*, 35(5):513–551, 2015.

[28] Tung-Chieh Chen and Yao-Wen Chang. Chapter 10 — Floorplanning. In Laung-Terng Wang, Yao-Wen Chang, and Kwang-Ting (Tim) Cheng, editors, *Electronic Design Automation*, pages 575–634. Morgan Kaufmann, 2009.

[29] Fan-Rong King Chung, Ronald Lewis Graham, Verner Emil Hoggatt, and Mark Kleiman. The number of Baxter permutations. *J. Comb. Theory, Ser. A*, 24:382–394, 1978.

[30] Jim Conant and Tim Michaels. On the number of tilings of a square by rectangles. *Annals of Comb.*, 18:21–34, 2014.

[31] Hubert de Fraysseix, Patrice Ossona de Mendez, and Pierre Rosenstiehl. Bipolar orientations revisited. *Discret. Appl. Math.*, 56(2-3):157–179, 1995.

[32] Denis Denisov and Vitali Wachtel. Random walks in cones. *Annals of Prob.*, 43(3):992–1044, 2015.

[33] Blanche Descartes. Division of a square into rectangles. *Eureka*, (34):31–35, 1971.

[34] Enrica Duchi and Corentin Henriet. A bijection between rooted planar maps and generalized fighting fish. arXiv:2210.16635, 2022.

[35] Serge Dulucq, S. Gire, and Olivier Guibert. A combinatorial proof of J. West's conjecture. *Discret. Math.*, 187(1-3):71–96, 1998.

[36] Serge Dulucq, S. Gire, and J. West. Permutations with forbidden subsequences and nonseparable planar maps. *Discret. Math.*, 153(1-3):85–103, 1996.

[37] Andrzej Ehrenfeucht and Grzegorz Rozenberg. T-structures, T-functions, and texts. *Theor. Comput. Sci.*, 116(2):227–290, 1993.

[38] David Eppstein, Elena Mumford, Bettina Speckmann, and Kevin Verbeek. Area-universal and constrained rectangular layouts. *SIAM J. Comput.*, 41(3):537–564, 2012.

[39] Wenjie Fang. Fighting Fish and Two-Stack Sortable Permutations. *Séminaire Lotharingien de Combinatoire*, 80B:P7, 2018. Proceedings of the 30th International Conference on "Formal Power Series and Algebraic Combinatorics", July 16 - 20, 2018, Dartmouth College, Hanover, USA.

[40] Stefan Felsner. Lattice structures from planar graphs. *Electron. J. Comb.*, 11(1), 2004.

[41] Stefan Felsner, Éric Fusy, Marc Noy, and David Orden. Bijections for Baxter families and related objects. *J. Comb. Theory, Ser. A*, 118(3):993–1020, 2011.

[42] Stefan Felsner and Lorenz Wernisch. Markov chains for linear extensions, the two-dimensional case. In *Proc. ACM-SIAM Symposium on Discrete Algorithms (SODA)*, pages 239–247. ACM/SIAM, 1997.

[43] Philippe Flajolet and Robert Sedgewick. *Analytic Combinatorics*. Cambridge University Press, 2009.

[44] Jean Françon and Gérard Viennot. Permutations selon leurs pics, creux, doubles montées et double descentes, nombres d'Euler et nombres de Genocchi. *Discret. Math.*, 28(1):21–35, 1979.

[45] Ryo Fujimaki, Youhei Inoue, and Toshihiko Takahashi. An asymptotic estimate of the numbers of rectangular drawings or floorplans. In *International Symposium on Circuits and Systems (ISCAS 2009), 24-17 May 2009, Taipei, Taiwan*, pages 856–859. IEEE, 2009.

[46] Ryo Fujimaki and Toshihiko Takahashi. A surjective mapping from permutations to room-to-room floorplans. *IEICE Trans. Fundam. Electron. Commun. Comput. Sci.*, 90-A(4):823–828, 2007.

[47] Éric Fusy. Transversal structures on triangulations: A combinatorial study and straight-line drawings. *Discret. Math.*, 309(7):1870–1894, 2009.

[48] Éric Fusy, Erkan Narmanli, and Gilles Schaeffer. Enumeration of corner polyhedra and 3-connected Schnyder labelings. *Electron. J. Comb.*, 30(2), 2023.

[49] Éric Fusy, Erkan Narmanli, and Gilles Schaeffer. On the enumeration of plane bipolar posets and transversal structures. *Europ. J. Combin.*, 116:103870, 2024.

[50] Emmanuel Guitter, Charlotte F. Kristjansen, and Jacob L. Nielsen. Hamiltonian cycles on random Eulerian triangulations. *Nuclear Phys. B*, 546(3):731–750, 1999.

[51] Youhei Inoue, Toshihiko Takahashi, and Ryo Fujimaki. Counting rectangular drawings or floorplans in polynomial time. *IEICE Trans. Fundam. Electron. Commun. Comput. Sci.*, 92-A(4):1115–1120, 2009.

[52] Richard Kenyon, Jason Miller, Scott Sheffield, and David B. Wilson. Bipolar orientations on planar maps and SLE_{12}. *Annals of Prob.*, 47(3):1240–1269, 2019.

[53] Shirley Law and Nathan Reading. The Hopf algebra of diagonal rectangulations. *J. Comb. Theory, Ser. A*, 119(3):788–824, 2012.

[54] Jean-Louis Loday. Realization of the Stasheff polytope. *Archiv d. Math.*, 83(3):267–278, 2004.

[55] Colin L. Mallows. Baxter permutations rise again. *Journal of Combinatorial Theory, Series A*, 27(3):394–396, 1979.

[56] Emily Meehan. Baxter posets. *Electon. J. Comb.*, 26(3):3, 2019.

[57] Emily Meehan. The Hopf algebra of generic rectangulations. arXiv:1903.09874, 2019.

[58] Arturo Merino and Torsten Mütze. Personal communication, 2021.

[59] Arturo Merino and Torsten Mütze. Combinatorial generation via permutation languages. III. Rectangulations. *Discrete Comput. Geom.*, 70(1):51–122, 2023.

[60] Folkert Müller-Hoissen, Jean Marcel Pallo, and Jim Stasheff, editors. *Associahedra, Tamari Lattices and Related Structures*. Progress in Mathematics. Birkhäuser, 2012.

[61] The On-Line Encyclopedia of Integer Sequences. Published electronically at http://oeis.org/.

[62] Vincent Pilaud and Francisco Santos. Quotientopes. *Bull. London Math. Soc.*, 51(3):406–420, 2019.

[63] Lionel Pournin. The diameter of associahedra. *Adv. Math.*, 259:13–42, 2014.

[64] James Propp. Lattice structure for orientations of graphs. arXiv:math/0209005, 1993.

[65] Nathan Reading. Lattice congruences of the weak order. *Order*, 21(4):315–344, 2004.

[66] Nathan Reading. Generic rectangulations. *Europ. J. Comb.*, 33(4):610–623, 2012.

[67] Sadiq M. Sait and Habib Youssef. *VLSI physical design automation: Theory and practice*. IEEE, 1995.

[68] Gilles Schaeffer. *Conjugaison d'arbres et cartes combinatoires aléatoires*. PhD thesis, Bordeaux 1, 1998.

[69] Ernst Schröder. Vier combinatorische Probleme. *Zeitschrift für Mathematik und Physik*, Band 15:361–376, 1870.

[70] Zion Cien Shen and Chris C. N. Chu. Bounds on the number of slicing, mosaic, and general floorplans. *IEEE Trans. Comput. Aided Des. Integr. Circuits Syst.*, 22(10):1354–1361, 2003.

[71] Naveed A. Sherwani. *Algorithms for VLSI physical design automation*. Kluwer, 1993.

[72] Daniel D. Sleator, Robert E. Tarjan, and William P. Thurston. Rotation distance, triangulations, and hyperbolic geometry. *J. Amer. Math. Soc.*, 1(3):647–681, 1988.

[73] Richard P. Stanley. Hipparchus, Plutarch, Schröder, and Hough. *The American Mathematical Monthly*, 104(4):344–350, 1997.

[74] Richard P. Stanley. *Catalan Numbers*. Cambridge University Press, 2015.

[75] James Dillon Stasheff. Homotopy associativity of H-spaces. I, II. *Trans. Amer. Math. Soc.*, 108:293–312, 1963. **108** (1963), 275-292; ibid.

[76] John Philip Steadman. *Architectural Morphology*. Pion, 1983.

[77] Toshihiko Takahashi and Ryo Fujimaki. Fujimaki–Takahashi squeeze: Linear time construction of constraint graphs of floorplan for a given permutation. *IEICE Trans. Fundam. Electron. Commun. Comput. Sci.*, 91-A(4):1071–1076, 2008.

[78] Toshihiko Takahashi, Ryo Fujimaki, and Youhei Inoue. A $(4n-4)$-bit representation of a rectangular drawing or floorplan. In Hung Q. Ngo, editor, *Proc. COCOON 2009*, volume 5609 of *LNCS*, pages 47–55. Springer, 2009.

[79] Dov Tamari. *Monoïdes préordonnés et chaînes de Malcev*. Université de Paris, Paris, 1951. Thèse.

[80] William Thomas Tutte. A census of planar triangulations. *Canadian J. Math.*, 14:21–38, 1962.

[81] William Thomas Tutte. A census of planar maps. *Canadian J. Math.*, 15:249–271, 1963.

[82] Marc J. van Kreveld and Bettina Speckmann. On rectangular cartograms. *Comput. Geom.*, 37(3):175–187, 2007.

[83] Gérard Viennot. A bijective proof for the number of Baxter permutations. *Séminaire Lotharingien de Combinatoire*, 1-3:28–29, 1981.

[84] Julian West. Generating trees and the Catalan and Schröder numbers. *Discret. Math.*, 146(1-3):247–262, 1995.

[85] Bo Yao, Hongyu Chen, Chung-Kuan Cheng, and Ronald L. Graham. Floorplan representations: Complexity and connections. *ACM Trans. Design Autom. Electron. Syst.*, 8(1):55–80, 2003.

[86] Doron Zeilberger. A proof of Julian West's conjecture that the number of two-stack-sortable permutations of length n is $2(3n)!/((n+1)!(2n+1)!)$. *Discret. Math.*, 102(1):85–93, 1992.